THE ROLE OF *IN UTERO* ENDOTOXIN EXPOSURE IN THE POSTNATAL IMMUNE RESPONSE IN MICE

By

Emilyn Constance Banfield

A dissertation submitted to Johns Hopkins University in conformity with the requirements for the degree of Doctor of Philosophy

Baltimore, Maryland

March 2020

Abstract

In this body of work, we were interested in both the temporary state of endotoxin tolerance and the gastrointestinal diseases known collectively as inflammatory bowel disease (IBD). Endotoxin tolerance is a state of muted immune response to bacterial endotoxins after an initial, sub-lethal exposure to an endotoxin. It has been observed primarily in sepsis patients of all ages and can lead to secondary infection and mortality. Conversely, IBD is a disease associated with increased inflammation and tissue damage within the gastrointestinal tract. Although early environmental influences are thought to influence disease development in IBD, little is known about the role of the uterine environment on subsequent early life endotoxin tolerance or IBD risk. We hypothesized that prenatal exposure to bacterial lipopolysaccharide (LPS), an endotoxin, could decrease responses to subsequent inflammatory triggers in early childhood. We also hypothesized that this exposure could modify the subsequent development of dextran sulfate sodium (DSS)-induced ulcerative colitis in adulthood by influencing the associated cellular and genetic immune response. To test our hypotheses, we exposed developing mice *in utero* to LPS or saline at embryonic day 17.5 (E17), and then induced either a second intraperitoneal exposure to LPS or saline in early life or colitis at 5 weeks and assessed inflammation and disease severity using a variety of metrics. In order to define the developmental impact of any LPS effect on colitis development, we also exposed one week old mice to either LPS or saline. Surprisingly, mice exposed to LPS at E17 were protected from subsequent colitis development, and maintained intestinal barrier and tight junction function similar to that of control mice that were not exposed to

DSS. By contrast, mice exposed to either LPS or saline at postnatal day 7 both developed severe colitis upon DSS exposure. These results identify a critical time window during fetal development during which exposure to an otherwise pro-inflammatory agent like LPS could protect against an inflammatory state in both early life and adulthood.

Primary Reader and Advisor: David Hackam, MD, PhD

Secondary Reader: Irina Burd, MD, PhD

Acknowledgements

I am incredibly grateful to my advisor, Dr. David Hackam, for enthusiastically supporting me throughout my thesis work. Dr. Hackam's insights, experience, and guidance have allowed me to learn what it means to be a thorough and careful scientist. I am also thankful to him for his patience as I worked through an extensive trial-and-error period both in the early years of my work and as I explored possible career options. He has always encouraged me to find the positive in each scientific failure and taken the time to brainstorm logical next steps, valuable lessons that I am sure to carry with me.

I am also thankful for the day-to-day mentorship of William "Benj" Fulton, who is one of the most knowledgeable and helpful scientists that I have ever met. He took my phone calls, text messages, and emails at all hours to help me troubleshoot difficult experiments and taught me many of the techniques I used to conduct my thesis work. His love for science and shoes have guided many before me and I'm sure many more students to come. I am forever indebted to him and all that he has done for me.

I would like to express my gratitude to Dr. Irina Burd, who allowed me to watch her perform countless intrauterine injections before embarking on my own experiments and served as a sounding board for necessary troubleshooting along the way. I would also like to thank Dr. Jill Fahrner, Dr. Kathleen Gabrielson, and Dr. Jonathan Pevsner for serving on my thesis committee and providing valuable feedback as well as insightful career advice.

Dedication

This thesis is dedicated to my mother, Marsha Banfield, who has been unwavering in her love and support throughout my academic journey. If everyone had someone like her to celebrate their successes, big and small, the world would be a kinder place.

Table of Contents

Abstract (Pg. ii)

Acknowledgements (Pg. iv)

Dedication (Pg. v)

List of Tables (Pg. x)

List of Figures (Pg. xi)

1. Introduction

a. Inflammatory bowel disease overview (Pg. 1)

b. Inflammatory bowel disease and development (Pg. 5)

c. Mouse models and methods of chemical induction of inflammatory bowel disease

i. Dextran sodium sulfate colitis model (Pg. 6)

ii. Other chemical induction of colitis models (Pg. 7)

iii. Chemically induced colitis severity measurements (Pg. 8)

iv. Measuring cellular changes at multiple time points (Pg. 8)

d. Immune response to endotoxins and bacterial ligands (Pg. 9)

e. Endotoxin tolerance (Pg. 10)

f. Ulcerative colitis and necrotizing enterocolitis (Pg. 11)

2. Development of intrauterine endotoxin model to study embryonic exposure to lipopolysaccharide and subsequent inflammatory bowel disease development

a. Intrauterine injection model (Pg. 13)

b. Use of CD-1 mice for intrauterine injection models (Pg. 14)

c. Hypothesis (Pg. 15)

3. Prenatal endotoxin exposure leads to early endotoxin tolerance in the ileum

a. Changes in cell type proliferation are a hallmark of endotoxin tolerance (Pg. 16)

b. Methods

i. Endotoxemia at P1 (Pg. 17)

ii. Quantitative real-time PCR transcriptomic analysis (Pg. 17)

iii. Immunofluorescence and histology (Pg. 17)

iv. Microscopy and fluorescence quantification (Pg. 18)

v. Statistical analysis (Pg. 18)

c. Prenatal LPS exposure lessens P1 immune response (Pg. 19)

d. Prenatal LPS exposure leads to increased cell proliferation after P1 LPS exposure (Pg. 19)

e. Prenatal LPS exposure has no effect on postnatal ileum architecture (Pg. 20)

f. The endotoxin tolerance observed at P1 disappears with time (Pg. 20)

g. Discussion (Pg. 31)

4. Prenatal exposure does not determine severity of necrotizing enterocolitis

a. Methods

i. Mouse model of necrotizing enterocolitis (Pg. 33)

ii. Quantitative real-time PCR and histology staining (Pg. 33)

iii. Statistical analysis (Pg. 34)

b. Prenatal LPS exposure does not cause a significant change in immune response to NEC in the ileum (Pg. 34)

c. No histological evidence of a difference in NEC severity between E17 LPS and E17 PBS groups (Pg. 35)

d. Discussion (Pg. 39)

5. Prenatal endotoxin exposure is protective against DSS colitis

a. Methods

i. Dextran sulfate sodium-induced colitis model in the mouse (Pg. 40)

ii. Mouse colonoscopy (Pg. 40)

iii. Quantitative real-time PCR (Pg. 41)

iv. Immunofluorescence and histology (Pg. 41)

v. Microscopy and fluorescence quantification (Pg. 41)

vi. 16S rRNA sequencing of microbes in mouse stool (Pg. 42)

vii. Statistical analysis (Pg. 42)

b. Prenatal LPS exposure protects mice from subsequent development of experimental colitis in adulthood (Pg. 43)

c. Prenatal exposure to LPS reduces the effects of colitis on weight loss and colon length (Pg. 44)

d. Prenatal LPS exposure leads to reduced inflammation and increased *Muc2* expression int he adult mouse colon (Pg. 46)

e. Prenatal LPS exposure minimizes the loss of goblet cells and tight junctions in adult mice with experimental colitis (Pg. 47)

f. Effects of *in utero* exposure to LPS on 16S rRNA sequencing of the microbiome (Pg. 49)

g. Discussion (Pg. 64)

6. Conclusions

a. Summary of significant findings (Pg. 68)

b. Future directions (Pg. 69)

7. **Bibliography** (Pg. 71)

List of Tables

3.1 Primers used for *in utero* plus early postnatal endotoxin exposure qRT-PCR experiments (Pg. 31)

5.1 Primers used for *in utero* plus 2% DSS exposure qRT-PCR experiments (Pg. 63)

List of Figures

2.1 An illustrated depiction of the general murine intrauterine injection model (Pg. ?)

3.1 Prenatal LPS exposure leads to endotoxin tolerance in the ileum immediately after birth (pg. 24)

3.2 Prenatal LPS exposure increases cell proliferation in the ileum among mice exposed to LPS immediately after birth (Pg. 25)

3.3 Prenatal LPS exposure does not alter ileum histology at postnatal day 1 (Pg. 26)

3.4 Endotoxin tolerance effects in the ileum due to prenatal LPS exposure lessen within the first week of life (Pg. 27)

3.5 Prenatal LPS exposure does not protect ileum integrity after postnatal day 7 LPS exposure (Pg. 28)

3.6 Endotoxin tolerance effects in the ileum due to prenatal LPS exposure largely disappear after ten days of life (Pg. 29)

3.7 Prenatal LPS exposure does not protect ileum integrity after postnatal day 10 LPS exposure (Pg. 30)

4.1 An illustrated depiction of the intrauterine injection plus four day necrotizing enterocolitis (NEC) exposure experimental model (Pg. 37)

4.2 Prenatal LPS exposure has no effect on the immune response associated with necrotizing enterocolitis (Pg. 38)

4.3 Prenatal LPS exposure does not protect against tissue degradation associated with necrotizing enterocolitis (Pg. 39)

5.1 An illustrated depiction of the intrauterine injection plus 2% DSS exposure experimental model (Pg. 51)

5.2 Mouse colonoscopy reveals that prenatal LPS exposure protects mice from subsequent development of experimental colitis in adulthood (Pg. 52)

5.3 Prenatal exposure to LPS reduces the effects of colitis on weight loss (Pg. 53)

5.4 Prenatal exposure to LPS reduces the effects of colitis on colon length (Pg. 54)

5.5 Postnatal exposure to LPS does not reduce the effects of colitis on colon length (Pg. 55)

5.6 Prenatal LPS exposure leads to reduced inflammation and increased *Muc2* expression in the adult mouse colon (Pg. 56)

5.7 Postnatal LPS exposure leads to inflammatory response in the adult mouse colon (Pg. 57)

5.8 Prenatal LPS exposure minimizes the loss of goblet cells in adult mice with experimental colitis (Pg. 58)

5.9 Prenatal LPS exposure minimizes the loss of tight junctions in adult mice with experimental colitis (Pg. 59)

5.10 LPS exposure at day 7 of age does not impact the colitis-induced loss of goblet cells and tight junctions in adult mice (Pg. 60)

5.11 Postnatal LPS exposure leads to typical loss of tight junctions in adult mice associated with experimental colitis (Pg. 61)

5.12 Effects of in utero LPS exposure on 16S rRNA sequencing of the microbiome (Pg. 62)

Chapter 1

Introduction

Inflammatory bowel disease overview

Inflammatory bowel disease (IBD), made up of the clinical subtypes ulcerative colitis and Crohn's disease, is characterized by episodes of excessive inflammation of the gastrointestinal tract. Both diseases typically have recurrent flares and remissions, with flare symptoms including abdominal pain, diarrhea, unintended weight loss, bloody stool, fatigue, and fever [1–3]. In cases of ulcerative colitis, the inflammation characteristic of disease is limited to the colonic mucosa, whereas Crohn's disease is characterized by transmural inflammation that can extend anywhere from the mouth to the anus [1,2,4,5]. For both diseases, diagnosis is a multi-step process. Blood tests can determine whether there is inflammation or anemia, the latter indicating potential internal bleeding [5]. They can also determine whether there are nutritional deficiencies, as they can indicate impaired absorption within the gastrointestinal tract. Stool can be checked using fecal occult blood tests for the presence of blood not visible to the eye [5]. Patients with symptoms suggestive of IBD often undergo colonoscopy, during which tissue biopsies are taken [1]. Mucosal biopsies of those with ulcerative colitis have thickened mucosa and architectural distortion of the colonic crypts. In Crohn's disease, noncaseating granulomas are the signature pathologic finding that is associated with disease [1,5,6]. Additional imaging (e.g. MRI) can be performed if needed.

Although the precise mechanisms leading to IBD remain incompletely understood, current thinking suggests that the disease stems from dysregulation of the immune response, epithelial barrier breakdown, and factors in the Western diet [1–4,7]. Specifically, the Western diet is characterized as being high in fat and sugar and low in fiber. This diet has been shown to alter the microbiome and subsequently cause reduced intestinal mucosal thickness, allowing for activation of the immune system by increasing intestinal permeability [8]. Interestingly, smoking is protective in ulcerative colitis, with primarily non- and former smokers affected, and is associated with increased disease in Crohn's disease [8,9]. Psychosocial stress has been shown to be associated with IBD, as stress causes the release of norepinephrine into the intestinal lumen, which then causes increased intestinal permeability and an associated immune response [10]. Additional known risk factors include being Caucasian or of Ashkenazi Jewish descent and being less than 30 years of age [3,11]. Previous studies have shown 6.3-17.0% concordance in monozygotic twins and 0.0-6.3% in dizygotic twins, indicating a strong genetic role in the development of ulcerative colitis [4,7,12]. Despite this clear association, incomplete concordance in monozygotic twins suggests that there are other factors at work in the development of ulcerative colitis.

The incidence of IBD in the US compared to other countries is high, with approximately 1.5 million people living with the disease [1,11,13]. For much of the 20th century IBD was considered a disease of the Western world, often isolated to industrial countries in Europe and North America. However, there is significant evidence indicating that as the number of industrialized countries increases globally, so too does the global incidence of ulcerative colitis and Crohn's disease [11,13–15]. With the highest reported

prevalence in North America occurring in the US (286 per 100,000), ulcerative colitis is the focus of this paper [2].

As stated above, ulcerative colitis is believed to be caused by a variety of factors, one of which is dysregulation of the immune system. The immune system is made up of both the innate immune system, a nonspecific defense mechanism, and the adaptive immune system, an antigen-specific defense mechanism. Within both systems, cytokines are secreted by immune cells and act through receptors to trigger an immune response [16]. Increased levels of the innate immune system-associated cytokines IL-6, IL-8, IL1β, and TNF-α and the adaptive immune system-associated cytokines IL-5, IL-13, IL-17, IL-22, and IFN-γ are associated with ulcerative colitis [17]. Increased expression of these proinflammatory cytokines leads to increased barrier permeability, decreased tight junction function, and increased epithelial cell apoptosis [2].

However, the immune response characteristic of ulcerative colitis is not limited to cytokines alone. Previous concordance studies have shown that heritability and genetic changes play a substantial part in inflammatory bowel disease, including ulcerative colitis etiology. In fact, over 200 risk loci have been identified with inflammatory bowel disease [4,18]. However, the identification of causal genes and specific loci associated with ulcerative colitis has not been as clearly defined a path as with Crohn's disease. Many GWAS studies focus on Crohn's disease, due in part to the fact that risk loci have been found on genes like *NOD2* and *ATG16L1*, genes well-established as being associated with the disease [4]. Despite this, GWAS studies have shown that risk loci near interleukin 23-associated genes and *IL-10* are associated with ulcerative colitis, with the former genes being associated with both IBD subtypes [2,4,17,19]. Similarly, expression

of *TLR4,* which binds to Gram-negative bacteria like lipopolysaccharide, is upregulated during active flare-ups, causing characteristic ulcers and tissue degradation [20,21]. Importantly, genes associated with production of tight junction proteins or mucin production (see below) have actively been studied instead, including the claudin-encoding genes of the same name that code for components of tight junctions [18,22].

In the healthy intestine, the intestinal epithelium serves as a selectively permeable barrier, protecting tissue from pathogens that populate the lumen upon ingestion, absorbing nutrients from ingested food, and allowing the transfer of fluids and electrolytes between the tissue and lumen [2,23,24]. This is achieved via intestinal epithelial cells, which act as a barrier and make up the lumen of the colon, goblet cells, which secrete mucin via MUC2 that acts as both a lubricant and is home to the intestinal microbiota, and tight junctions, which allow for selective passage of nutrients through the intestinal barrier [23–25]. However, in ulcerative colitis, the intestine breaks down and loses its selective permeability, instead allowing microbial pathogens to attack the colon and subsequently cause inflammation and disrupting the flow of fluids and electrolytes. The latter consequence can lead to diarrhea, which is a symptom in almost all cases of ulcerative colitis [26]. Epithelial breakdown is also due, in part, to a loss of tight junctions due to a decrease in the number of ZO-1 proteins present in the tissue and reduced goblet cell function via decreased expression of *mucin 2 (MUC2)* [23,27].

One of the factors associated with IBD development has proven to be the host-microbe interaction in the mucosal layer of the intestine. Approximately 99% of the microbiome is made up of the phyla *Firmicutes, Bacteriodetes, Proteobacteria,* and *Actinobacteria* [28]. In healthy adults, the two dominant phyla are *Firmicutes* and

Bacteriodetes. Most of these bacteria reside in the distal small intestine and the colon and bind to intestinal epithelial cells, creating a protective biofilm of bacteria on the luminal surface of the colon [28,29]. Ordinarily, the gut microbiome performs a variety of beneficial tasks. These bacteria synthesize essential vitamins and short-chain fatty acids, help the mucosal immune system to mature, and contribute to host defense by preventing pathogen colonization [28,29]. However, alterations in diversity can lead to disruptions in immune function and reduced regulation of pathogenic colonization. These alterations can be due to a variety of environmental factors, including diet, smoking, and antibiotic use [30]. In ulcerative colitis, there is a decrease in the overall diversity and number of beneficial bacteria and increase in populations of harmful bacteria in the colon [1,29]. For example, studies have shown that *Akkermansia muciniphila,* which makes up between 1-5% of the human microbiome, is decreased in ulcerative colitis [31,32]. In addition to disrupting the prevention of pathogenic bacterial colonization, these microbiotic changes lead to mucosal barrier and epithelial cell damage, allowing harmful bacteria to come in contact with the tissue and cause additional inflammation and disease [29].

Inflammatory bowel disease and development

A growing body of evidence has shown that a variety of environmental exposures *in utero* have an effect on neonatal development. Previous studies have shown that maternal diet supplementation during pregnancy with methyl donor micronutrients can increase ulcerative colitis susceptibility in mouse offspring [33,34]. Though these results might suggest that exposure to mother and fetus are one in the same, Hemmerling *et al.* showed that maternal inflammation did not affect the risk of inflammatory bowel disease

in mouse pups, nor did it affect the microbiome of the newborn pups, giving evidence that localized antenatal inflammation during pregnancy plays a critical role in development. Consistent with this idea, it has been shown that full-term and preterm infants who had different immune responses immediately after birth quickly developed similar responses. These responses differed greatly from infants that received an inflammatory exposure during this time of immune response convergence [35]. This ability to alter the immune response points to a critical exposure window for immune system development, though the long-term role of a localized environmental exposure on the developing fetus remains unknown.

Mouse models and methods of chemical induction of inflammatory bowel disease

There are three well-established, commonly used methods to chemically induce IBD in mice: dextran sodium sulfate (DSS) administration in an acute or chronic fashion, 2,4,6-Trinitrobenzenesulfonic acid (TNBS) administration, and oxazolone administration. All three models mimic the intestinal inflammation characteristic of ulcerative colitis via administration of drugs that cause damage to the intestinal epithelium.

Dextran Sodium Sulfate Colitis Model

A widely used model is the DSS colitis model, as it is simple, reproducible, and rapid. DSS is a negatively charged, water-soluble sulfated polysaccharide that breaks down the protective epithelial layer of the colon, exposing the tissue to bacteria and other pro-inflammatory agents within the lumen though the exact mechanism of this inflammation induction remains unknown. To mimic human disease, 40-50 kDa DSS is

administered via the drinking water of mice. In the acute colitis model, this administration occurs over a short (e.g. seven days) period while in the chronic model, administration of DSS occurs over a longer period of time. Because it is an anticoagulant, DSS colitis promotes intestinal bleeding. Additional clinical signs of disease include alternation of tight junction protein expression, increased proinflammatory cytokine production, weight loss, diarrhea, bloody stool, goblet cell depletion, and shortening of the colon. The acute model is useful when studying the role of the innate immune system in ulcerative colitis and intestinal inflammation as T and B cells are not required to develop colitis in the murine DSS model. It is important to note that DSS dose and subsequent susceptibility to disease depends on the mouse strain used in the model, as some strains are more susceptible than others to developing chemically-induced ulcerative colitis.

Other Chemical Induction of Colitis Models

TNBS and oxazolone are both haptic agents, requiring dilution in 50% ethanol in order to break the epithelial barrier. Both methods require a pre-sensitization step in which mice are exposed to a small amount of TNBS or oxazolone in an acetone/olive oil mixture on shaved skin on Day 1 of the model. At a later date, usually Day 8 of the model, a catheter is used to administer an intra-rectal exposure to the pre-sensitized drug. Both TNBS and oxazolone mimic the inflammatory state seen in IBD by binding to high molecular weight proteins, causing those proteins to become immunogenic. However, TNBS induces a Th1-based inflammatory response in which Th1 signals cause CD4 T cell and pro-inflammatory cytokine (e.g. TNFα) infiltration into the colon. Though it is

used to model the inflammation associated with ulcerative colitis, it more closely mimics the gene expression and immune changes of Crohn's disease. In contrast, oxazolone induces a Th2-based inflammatory response that, when administered rectally, closely mimics ulcerative colitis.

Chemically-Induced Colitis Severity Measurements

Regardless of the method used for colitis induction, there are two gold standard measurements used to measure colitis severity in mice: weight change throughout the model and colon length at the end of the model. To measure weight change associated with colitis, mice are weighed each day of the model until euthanization, where mice are weight before the colon is removed and measured. After euthanization and a laparotomy that exposed the intestinal tissue, the colon is removed with surgical scissors at the anus and the distal small intestine, where the small intestine meets the cecum. The tissue is then measured from the proximal colon to the end of the colon.

Measuring Cellular Changes at Multiple Time Points

To study the effect of *in utero* bacterial endotoxin exposure on the postnatal immune system, we used a variety of measurements at several time points (see **Chapters 3-5**) to establish whether any effects were time-sensitive. We exposed mice *in utero* to LPS or PBS (2 mg/kg) and then the mouse pups received a second exposure to LPS (2 mg/kg) at day one of life (P1) via intraperitoneal injection to mimic early postnatal infection (**Chapter 3**). We repeated this experiment with mice at P7 and P10,

respectively, to mimic postnatal infections at various time points as the postnatal immune system develops (**Chapter 3**).

Though important information can be gleaned from the above experiments, we saw the importance of putting any potential findings into a disease context for translational purposes and thus repeated the *in utero* exposure but, at P7, began a three day model of necrotizing enterocolitis using a previously published model developed and validated by our lab (**Chapter 4**).

In addition to these early postnatal experiments, mice exposed to *in utero* LPS or PBS were exposed at five weeks to a six-day 2% DSS colitis model (see **Chapter 5**) to determine whether *in utero* endotoxin exposure caused an immunologic change that persisted into adulthood. In these experiments, it was important to establish whether any observed effects were due to prenatal exposure or merely an exposure at any point prior to the start of the DSS model. To assess this, we also conducted experiments in which no *in utero* exposure was performed but instead LPS or PBS was delivered via intraperitoneal injection at P7 and then the DSS model was performed at five weeks.

Immune Response to Endotoxins and Bacterial Ligands

Bacterial endotoxins, primarily made up of LPS, are found in the cell wall of Gram-negative bacteria like *Escherichia coli* and *Helicobacter pylori* and are secreted without harm to the bacterial cell wall. Exposure to bacterial endotoxins results in a cellular stress response in which pro-inflammatory cytokines like IL-6, IL1β, and TNF-α and other cellular stress markers like nitric oxide are released via the TLR4/MyD88 pathway [36]. *TLR4* plays a crucial role as an agonist in the innate immune response by

binding, in an intramembrane complex along with CD14, MD-2, and LPS-binding protein, to LPS, which triggers an oligomerization of the TLR4 protein and recruits myeloid differentiation primary response gene 88 (MyD88) [36]. Recruitment of MyD88 leads to downstream activation of nuclear factor-κB, signaling an inflammatory response and apoptosis. Consistent with this, in 1990, van Deventer *et al.* found that healthy volunteers given lipopolysaccharide developed symptoms including fever and pro-inflammatory cytokine release [37]. As such, LPS is used widely in the laboratory both *in vivo* and *in vitro* to mimic a bacterial infection, allowing for the study of the infection-related immune response.

Endotoxin Tolerance

Endotoxin tolerance was first described in 1946 by Paul Beeson, who noted that rabbits that received daily typhoid vaccine exposure did not develop a typical fever response [38–40]. It is now defined as hypo-responsiveness upon exposure to a lethal dose of endotoxin, often lipopolysaccharide, after an earlier exposure to endotoxin. In their foundational 1969 paper, Greisman and Hornick identified two distinct phases of endotoxin tolerance: early phase and late phase [41]. In early phase tolerance, there is no antibody-dependence nor endotoxin specificity and macrophages play a critical role [38,41]. In late phase tolerance, there is anti-"O" antibody and endotoxin specificity, which curtail the release of macrophages [38,41]. This hypo-responsiveness is a temporary state, with reports of normal responsiveness returning between 8-14 days [38,39]. Specifically, peak hypo-responsiveness occurs within 48 hours of the second endotoxin exposure in early phase tolerance and after 48 hours of the second exposure in

late phase tolerance [41]. During this time, regardless of phase, expression of the proinflammatory cytokines TNFα and IL1β is reduced [42]. In fact, TNFα is considered the best marker for endotoxin tolerance as it is normally highly expressed upon LPS exposure and is nearly universally inhibited across *in vivo* and *in vitro* studies [38]. However, not all cytokines act in this manner. Multiple studies have shown that IL-6 expression is increased in the endotoxin tolerant state [38,43,44]. Cytokine expression is not the only change seen in this state of hypo-responsiveness. Nomura *et al.* showed that *Tlr4* expression is down-regulated in endotoxin tolerant mice [45]. As such, the Tlr4-MyD88 pathway cannot have a typical downstream effect on NF-κB and subsequent inflammation. Though there is still much to be learned about the mechanism involved in endotoxin tolerance, it is clear that it plays an important role in prevention of mortality in endotoxin-related diseases like sepsis [38,40,42].

Ulcerative Colitis and Necrotizing Enterocolitis

Necrotizing enterocolitis (NEC) is the leading cause of gastrointestinal-related death among premature neonates. NEC occurs in approximately one in 500 live births in the United States and though there is an increase in disease among African American male babies likely due to confounding factors, there is no clear association with sex or race/ethnicity [46]. However, there are known risk factors including prematurity, improper bacterial colonization after birth, and formula feeding [46,47]. Though these risk factors are well-known, no individual risk factor is sufficient nor necessary to cause disease. As such, NEC onset is often unpredictable, in some cases quickly and others slow and gradual, and reliable diagnosis does not occur until later stages of disease [48].

Similar to ulcerative colitis, NEC is characterized by an increase in proinflammatory cytokine production, decrease in goblet cell function, decrease in tight junction maturity, and increase in *TLR4* expression in both the intestinal epithelial cells as well as the intestinal crypts [49]. The impact of prematurity on development of these cellular changes cannot be overstated. The premature intestine has increased expression of *TLR4* due to the role *TLR4* plays in normal intestinal development via Notch signaling [46,47]. In full-term neonates, this expression is greatly reduced around the time of delivery and slowly increases as the immune system matures. However, high levels of *TLR4* expression in the already vulnerable premature neonate, along with other factors outlined above, make the intestine vulnerable to stress in the endoplasmic reticulum, increasing the amount of apoptosis and necrosis within the ileum [46,47,49].

Though these two diseases share many similarities, they are vastly different in key aspects of disease etiology. Perhaps the most important difference between the two is that ulcerative colitis is limited to the colon and necrotizing enterocolitis occurs in the ileum [2,3,46,47,49]. Ulcerative colitis affects the colon of adults before the age of 30, though incidence can also occur later in life after age 60 [1,3]. NEC, however, primarily affects the ileum of premature neonates. There is an inverse association between age at birth and disease severity but disease occurs within the first months of life [46,47]. Ulcerative colitis is characterized by periods of relapses (e.g. flare-ups) and remissions while NEC is characterized by the acute development of sepsis and subsequent tissue death among approximately 30% of all cases [49]. In addition, ulcerative colitis leads to reduced mucosal thickness and crypt abscesses but NEC is associated with mucosal thickening [49].

Chapter 2

Development of intrauterine endotoxin model to study embryonic exposure to lipopolysaccharide and subsequent IBD development

Intrauterine Injection Model

Pregnant CD-1 mice, which normally deliver pups at day 19-21 days of gestation, were used for this model, which was adapted from Burd *et al.* and is outlined in **Figure 2.1** [50]. Surgery was performed on day 17 of gestation. Isoflurane anesthesia was used in an induction chamber to anesthetize the pregnant mice; a nose cone attached to the isoflurane anesthesia was used to anesthetize the mice during surgery. Upon anesthetization, a mini laparotomy was performed on the pregnant mouse's abdomen. The cervix was then located and the two gestational sacks to the left of the cervix were exposed. LPS (Sigma-Aldrich L3129) at 2 mg/kg was injected into the uterine wall between the gestational sacks. Sterile saline was used to wash the gestational sacks before they were placed back in the abdomen. The fascia was then closed with vicryl sutures (Ethicon 3-0 Braided Vicryl Sutures) and the skin was closed with staples (Fine Science Tools, 9mm AutoClip). The mice were closely monitored for the preterm birth of pups. Controls for this experiment include surgery and injection of phosphate buffered saline (PBS) and sham surgery. All pups were weaned at three weeks of age and separated by sex.

Use of CD-1 Mice for Intrauterine Injection Models

CD-1 mice were purchased from Charles River Laboratories (Wilmington, MA) and bred in-house. Animal protocols were approved by the Johns Hopkins University Animal Care and Use Committee (protocol M017M304). They were housed in a pathogen-free environment on a 12-hour light/12-hour dark cycle and given free access to standard rodent chow (PicoLab mouse diet 20, 22% kcal % fat) and acidified tap water after weaning before beginning the DSS model. Mice that did not undergo the DSS model and were instead euthanized at P2, P8, or P11 were left with their mothers after birth in the cage conditions described above. Mice were bred beginning at nine weeks of age and removed from the breeding colony after six months.

Attempts were made at the beginning of this work to use C57BL/6 mice, as they are one of the most commonly used strains and many established knockout mice have a C57BL/6 background. However, these mice were unable to survive the intrauterine injection model and all pups of mice that underwent the model were either stillborn or died shortly after birth. Work then shifted to the use of CD-1 mice, which are historically common in the intrauterine injection model despite it being a less commonly used strain. CD-1 mice are used in this model for a variety of reasons. Unlike inbred C57BL/6 mice, they are an outbred strain, which means they accurately recapitulate the inter-individual variability seen in human disease and are often more robust than inbred strains. This is an especially important consideration when modeling ulcerative colitis, which has a range of severity from mild, localized disease to pancolitis, which affects the entire colon. They also produce large litters (between 12-16 pups) which ensures a higher likelihood of pups surviving the injection and being born alive to be used in a later model.

Hypothesis

We hypothesize that *in utero* exposure to inflammation will decrease responses to subsequent inflammatory triggers in both children and adults by altering expression of related IBD genes, protecting them from excessive inflammation and pain.

Chapter 3

Prenatal endotoxin exposure leads to early endotoxin tolerance in the ileum

Changes in cell type proliferation are a hallmark of endotoxin tolerance

As outlined in **Chapter 1**, endotoxin tolerance occurs when cells are exposed to a sub-lethal amount of endotoxin (e.g. LPS) and then enter a state of unresponsiveness upon subsequent LPS exposure. It is characterized by significantly downregulated proinflammatory cytokine expression as well as a significant reduction in apoptotic activity. Interestingly, endotoxin tolerance is also characterized by a redirection of biological processes in which cell proliferation is dependent on cell type. Ordinarily, exposure to LPS leads to a Toll-like receptor 4 (TLR4)-mediated T-cell response in which proinflammatory cytokine production increases, inducing the characteristic inflammatory response associated with bacterial exposure. During this time, Th17 proliferation greatly increases. In contrast, endotoxin tolerance is associated with increased cell proliferation of metallothioneins, cells associated with detoxification and reducing inflammation. In addition, Andrade *et al.* showed that endotoxin tolerance induced in male C56BL/6 mice led to increases Treg proliferation in the spleen, which is consistent with the state of reduced inflammation characteristic of endotoxin tolerance [51].

Methods

Endotoxemia at P1

At P1, CD-1 pups that were delivered spontaneously after an intrauterine injection of LPS at E17 (**Figure 2.1**) were given an intraperitoneal injection of LPS (L3129) at 2 mg/kg or PBS (0.9% Sodium Chloride, Hospira Inc.). They were then returned to their mother and euthanized 24 hours after injection. At euthanization, ileum samples were taken and either placed in 4% paraformaldehyde (Electron Microscope Services, Cat #RT15700) in PBS overnight or flash-frozen in liquid nitrogen and stored at -80 °C.

Quantitative real-time PCR transcriptomic analysis

RNA was extracted from ileum tissue using an Rneasy Mini Kit (Cat #74106, Qiagen) and converted into complementary DNA using a QuantiTect Reverse Transcription Kit (Cat #205314, Qiagen). Quantitative real-time PCR was performed on the Bio-Rad CFX96 Real-Time System using primers (**Tables 3.1**) relative to the housekeeping gene ribosomal protein large P0 (RPL0).

Immunofluorescence and histology

Ileum samples were collected immediately after euthanasia and fixed in 4% paraformaldehyde (Electron Microscope Services, Cat #RT15700) in PBS overnight. The tissue was then processed using a Microm STP 120 Spin Tissue Processor (Thermo Scientific), embedded in paraffin, and 5-µm thick sections were cut using a CUT 6062 microtome (SLEE). The paraffin-embedded ileum samples were probed with primary antibodies in a 1:200 dilution in TBST overnight at 4^0 C and probed with 4',6-diamidino-2-phenylindole (DAPI), anti-Ki67 (Abcam, Cat# 15580-100), and Alexa Fluor 488

donkey anti-rabbit at 1:1000 for two hours at RT then washed and mounted in Gelvatol mounting media. For hematoxylin and eosin (H & E) staining, the collection, fixation, and section cutting processes outlined above were used. The paraffin-embedded ileum samples were probed with hematoxylin stain for fifteen minutes and eosin stain for fifteen seconds at room temperature then washed and mounted using Permount mounting media (Fisher Scientific).

Microscopy and fluorescence quantification

All immunofluorescence images were acquired using a Nikon Eclipse Ti microscope with a Nikon A1 confocal laser microscope system. Images were captured using a 20X objective (Nikon Plan Apo 20x/0.75 DIC N2) and maximum intensity z-projections of 3-6 3 μm optical sections. The images were then analyzed using Fiji, quantified using Excel, and visual representations were created using GraphPad Prism 7. All H & E images were acquired using a Leica DMi8 inverted microscope. Images were captured using a 20X objective (Leica HC PLAN 20X/0.70). The images were analyzed using Fiji and visual representations were created using GraphPad Prism 7.

Statistical analysis

Data were analyzed using GraphPad Prism 7 software. All data were analyzed for significance using a one-way ANOVA test and post hoc Bonferroni correction for multiple comparisons. Statistical significance was determined by a p-value of <0.05. All PCR was performed in triplicate, with at least five pups in each experimental group. Data was assembled and graphed using GraphPad Prism 7.

Prenatal LPS exposure lessens P1 immune response

To determine whether *in utero* LPS exposure had an effect on the postnatal immune system, we first performed qRT-PCR on ileum tissue from P2 mice (**Table 3.1**) and analyzed pro-inflammatory cytokines Tnfα and *IL1*β. These results showed a significant increase in Tnfα and expression among mice exposed to E17 PBS plus P1 LPS compared to those that received E17 PBS, E17 LPS, and E17 LPS plus P1 LPS (**Figure 3.1A**). This expression pattern was also found in *IL1*β, where E17 PBS plus P1 LPS mice had significantly greater expression compared to all other groups (**Figure 3.1B**). Consistent with these results, analysis of p53 up-regulated modulator of apoptosis (PUMA) showed a significant increase in expression among the E17 PBS plus P1 LPS group compared to the E17 PBS, E17 LPS, and E17 LPS plus P1 LPS groups (**Figure 3.1C**).

Surprisingly, *Toll-like receptor 4* (*Tlr4*) expression was not significantly different between mice that received E17 PBS plus P1 LPS and mice that received E17 LPS but there was a significant increase in expression among E17 PBS plus P1 LPS mice compared to the E17 PBS and E17 LPS plus P1 LPS groups (**Figure 3.1D**). Taken together, these results suggest potential endotoxin tolerance within the ileum of in mice exposed to E17 LPS plus P1 LPS. To investigate effects of *in utero* LPS exposure beyond expression, we next performed immunostaining to determine whether there were any changes in basic cell function within the ileum.

Prenatal LPS exposure leads to increased cell proliferation after P1 LPS exposure

In order to evaluate the effect of this muted immune response among E17 LPS plus P1 LPS exposed mice, we next quantified the amount of cell proliferation within the ileum at P2. As shown in **Figure 3.2A-B**, mice exposed to E17 LPS plus P1 LPS had significantly more cell proliferation than all other groups. Upon examination, Ki67 positive cells were largely concentrated in the crypts of E17 LPS plus P1 LPS ilea, indicating potential for incorporation into intestinal villi. These results reveal that E17 LPS exposure leads to a significant increase in cell proliferation in intestinal crypts upon postnatal exposure to LPS and indicates a role for proliferation that is not directly involved in immune response. We next sought to determine whether there were any histological changes between exposure groups.

Prenatal LPS exposure has no effect on postnatal ileum architecture

To determine whether increased cell proliferation, decreased apoptosis, and decreased expression of immune markers like *Tlr4* had an effect on ileum integrity, we performed H & E staining on all exposure groups. As shown in **Figure 3.3A-B**, we found no significant difference between groups for mucosal thickness nor for villi length. Together with our results obtained by performing qRT-PCR, we found evidence of a muted immune response and a potential change in overall function for cell proliferation among mice exposed to E17 LPS plus P1 LPS. Of interest, this does not manifest in gross histological changes with potential long-term consequences for barrier function and absorption.

The endotoxin tolerance observed at P1 disappears with time

Endotoxin tolerance is a temporary state of incapacity in which cells cannot mount a proper immune response. This state can last for variable amounts of time and, as such, it was essential to our understanding of the role of prenatal LPS exposure on postnatal endotoxin tolerance that we perform the above experiments at multiple time points. As such, we performed qRT-PCR and histology staining on mice that were exposed to LPS or PBS at E17 and again at P7 or P10 via intraperitoneal injection.

Mice exposed to E17 LPS plus P7 LPS again showed a similar immune response to mice not exposed to LPS at P7. E17 PBS plus P7 LPS exposed mice had a significant increase in *IL1*β (**Figure 3.4B**). However, Tnfα expression did not follow the same pattern. Instead, the only significant difference was between the E17 PBS plus P7 LPS exposed group and the E17 LPS exposed group (**Figure 3.4A**).

When both PUMA and *Tlr4* expression were measured, there was no significant difference between groups (**Figure 3.4C-D**). Despite this and more consistent with proinflammatory cytokine expression, H & E staining revealed a breakdown of tissue integrity in both the E17 PBS plus P7 LPS and E17 LPS plus P7 LPS groups (**Figure 3.5**) compared to mice exposed to either E17 PBS or E17 LPS only. Together, these results suggest that at P7, the effects of early life endotoxin tolerance begin to wane within the first week of life in the mouse.

When the same experiments were conducted with intraperitoneal injections at P10, there was further evidence of a reduction in endotoxin tolerance. There was no significant difference in *IL1*β expression between E17 PBS plus P10 LPS and any other group (**Figure 3.6B**. Similarly, Tnfα expression was significantly different only between E17 PBS plus P10 LPS and E17 LPS exposed mice (**Figure 3.6A**). PUMA expression

patterns across groups were also different than those observed in the E17 plus P1 experiments. There was a significant increase in PUMA expression among E17 LPS plus P10 LPS exposed mice compared to E17 PBS plus P10 LPS exposed mice but there was a significant decrease in expression among E17 PBS and E17 LPS exposed mice compared to the same group (**Figure 3.6C**). Despite this increase in apoptosis, *Tlr4* expression was significantly reduced among E17 LPS plus P10 LPS exposed mice compared to E17 PBS plus P10 LPS exposed mice and was more similar to mice exposed only to E17 PBS (**Figure 3.6D**). This result was surprising given the expression of proinflammatory cytokines outlined above. As such, it was necessary to again perform histological staining to determine whether the expression patterns we observed among mice exposed to P10 LPS had an effect on tissue integrity.

Consistent with our inflammatory marker qRT-PCR results, H & E staining showed a further disruption of both tissue and villi integrity within both the E17 PBS plus P10 LPS and E17 LPS plus P10 LPS exposed mice (**Figure 3.7**) compared to mice exposed to only E17 PBS or E17 LPS.

Taken as a whole, these findings show that, when exposed to *in utero* LPS, there is a critical exposure window in mice during which a second, postnatal LPS exposure can have an suppressive effect on immune response. This finding is consistent with the known temporary state of endotoxin tolerance and provides further insight into the role of *in utero* exposure on postnatal immune response. Though this has shown to be a temporary state, it can have significant implications for development of early postnatal diseases like sepsis.

Figure 3.1. ***Prenatal LPS exposure leads to endotoxin tolerance in the ileum immediately after birth.*** qRT-PCR measurements from ileums of mice that were exposed to either LPS (2 mg/kg) or PBS at E17 and then LPS again at postnatal day 1 (P1). Each gene is indicated above the graph, each point represents an individual mouse, and all expression levels are relative to RPL0 expression. $n \geq 7$ animals analyzed per group. All data is representative of three separate experiments and one-way ANOVA tests were performed to determine significance.

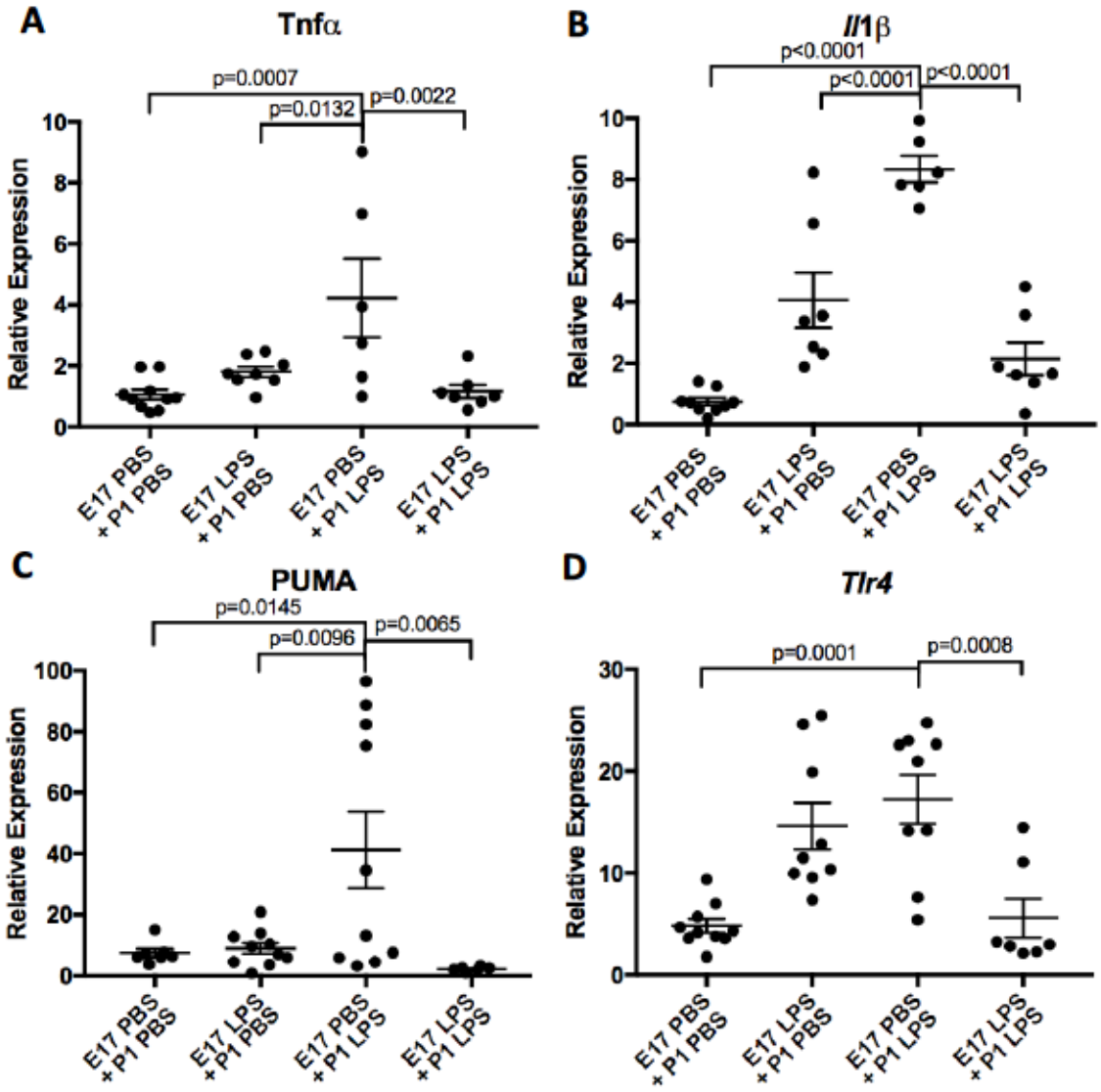

Figure 3.2. ***Prenatal LPS exposure increases cell proliferation in the ileum among mice exposed to LPS immediately after birth.*** (**A**) Representative confocal micrographs of the ileums of mice exposed LPS (2 mg/kg) or PBS at E17 and subsequently exposed to LPS at postnatal day 1 (P1). (**B**) Quantification of relative fluorescence measurements of KI-67 staining compared against DAPI staining. $n \geq 2$ per group. All data is representative of three separate experiments and one-way ANOVA tests were performed to determine significance.

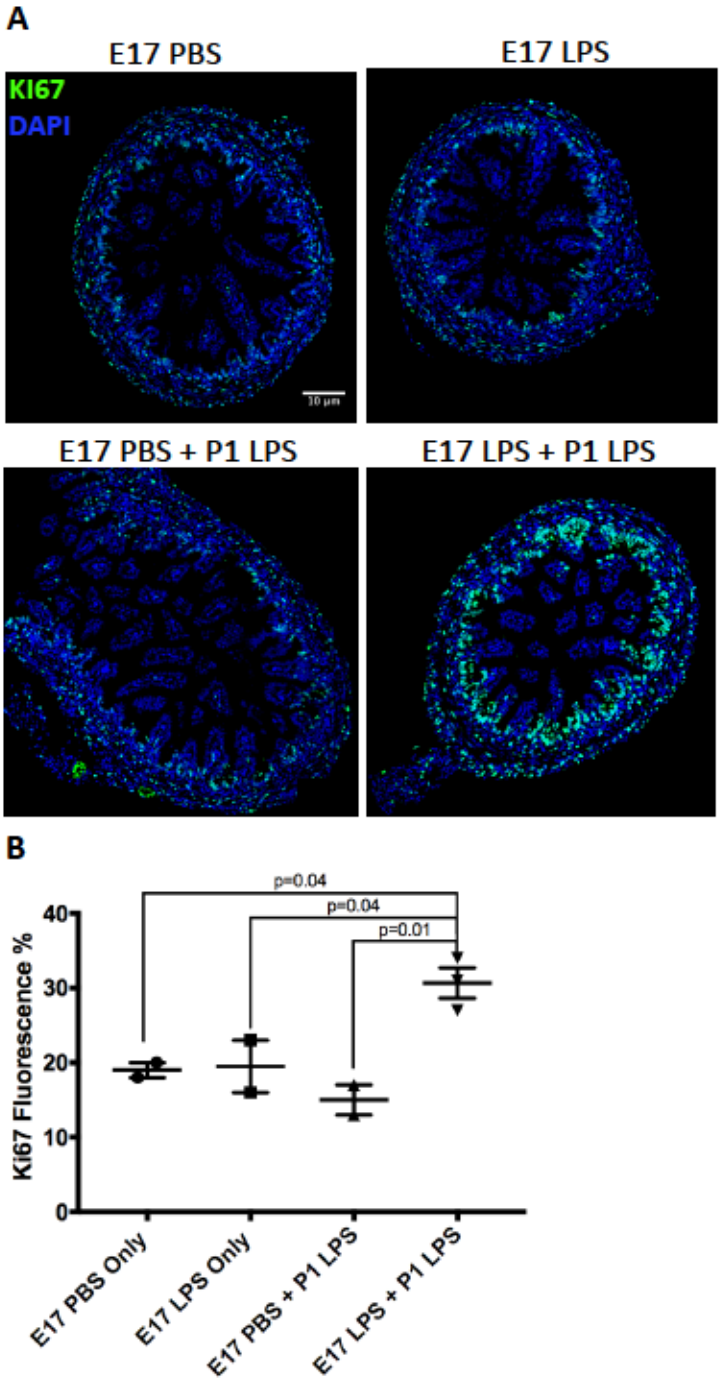

Figure 3.3. ***Prenatal LPS exposure does not alter ileum histology at postnatal day 1.*** (**A**) Representative micrograph of H & E staining in the ileum of mice that were exposed to either LPS (2mg/kg) or PBS at E17 and LPS at postnatal day 1 (P1). All data is representative of three separate experiments (n ≥ 3 per group, per experiment).

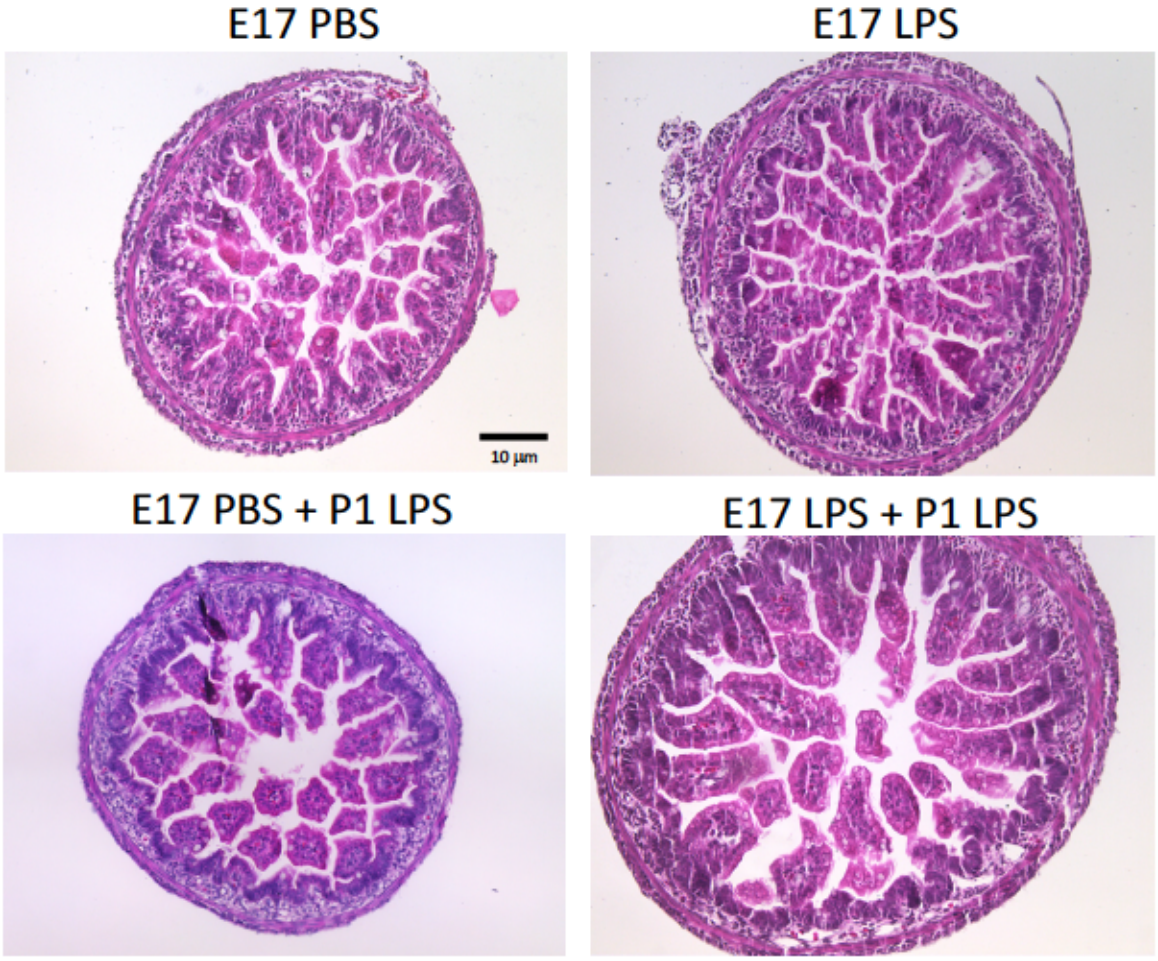

Figure 3.4. ***Endotoxin tolerance effects in the ileum due to prenatal LPS exposure lessen within the first week of life.*** qRT-PCR measurements from ileums of mice that were exposed to either LPS (2 mg/kg) or PBS at E17 and then LPS again at postnatal day 7 (P7). Each gene is indicated above the graph, each point represents an individual mouse, and all expression levels are relative to RPL0 expression. $n \geq 54$ animals analyzed per group. All data is representative of three separate experiments and one-way ANOVA tests were performed to determine significance.

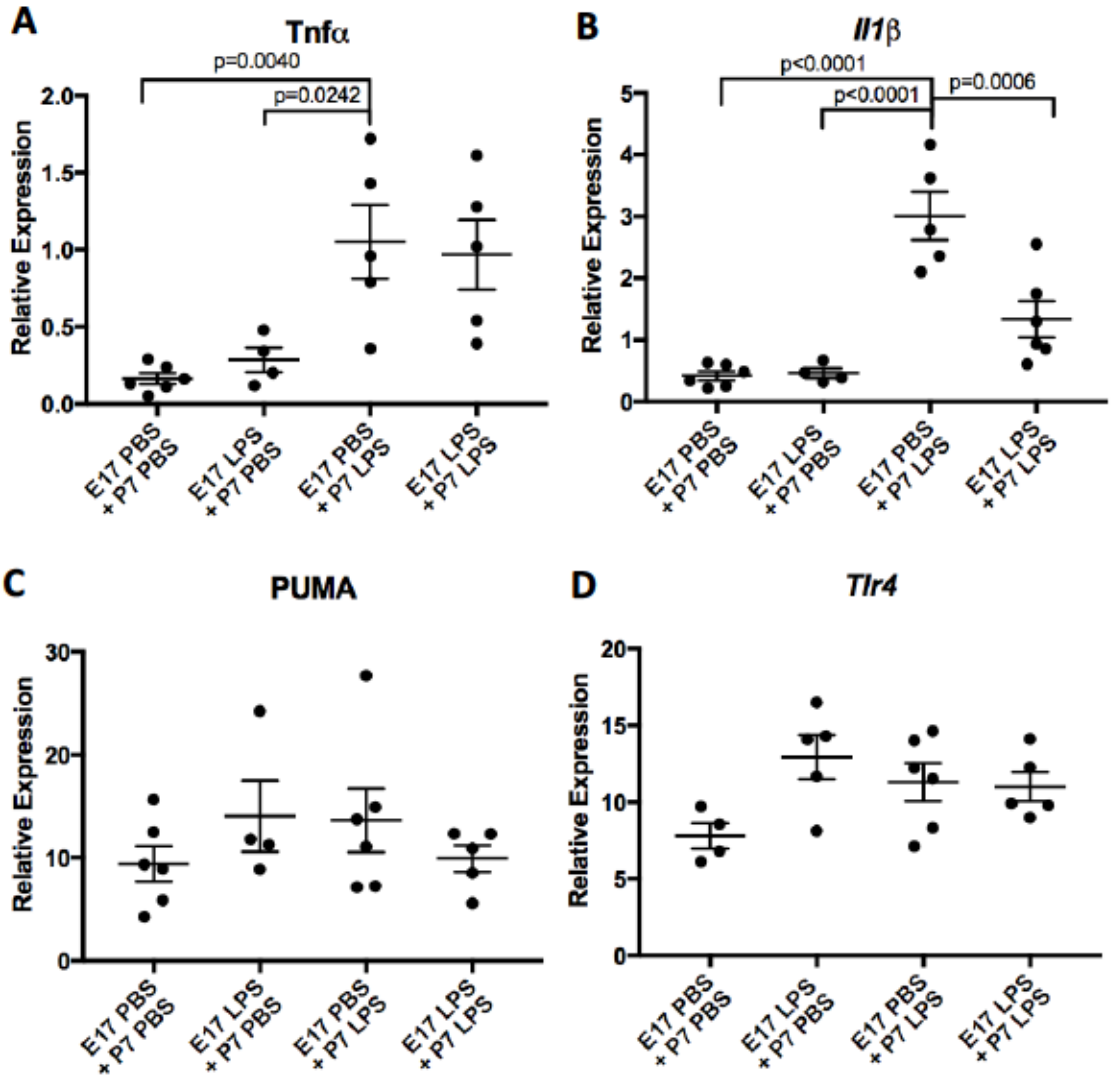

Figure 3.5. ***Prenatal LPS exposure does not protect ileum integrity after postnatal day 7 LPS exposure.*** **(A)** Representative micrograph of H & E staining in the ileum of mice that were exposed to either LPS (2mg/kg) or PBS at E17 and LPS at postnatal day 7 (P7). All data is representative of three separate experiments (n ≥ 4 per group, per experiment).

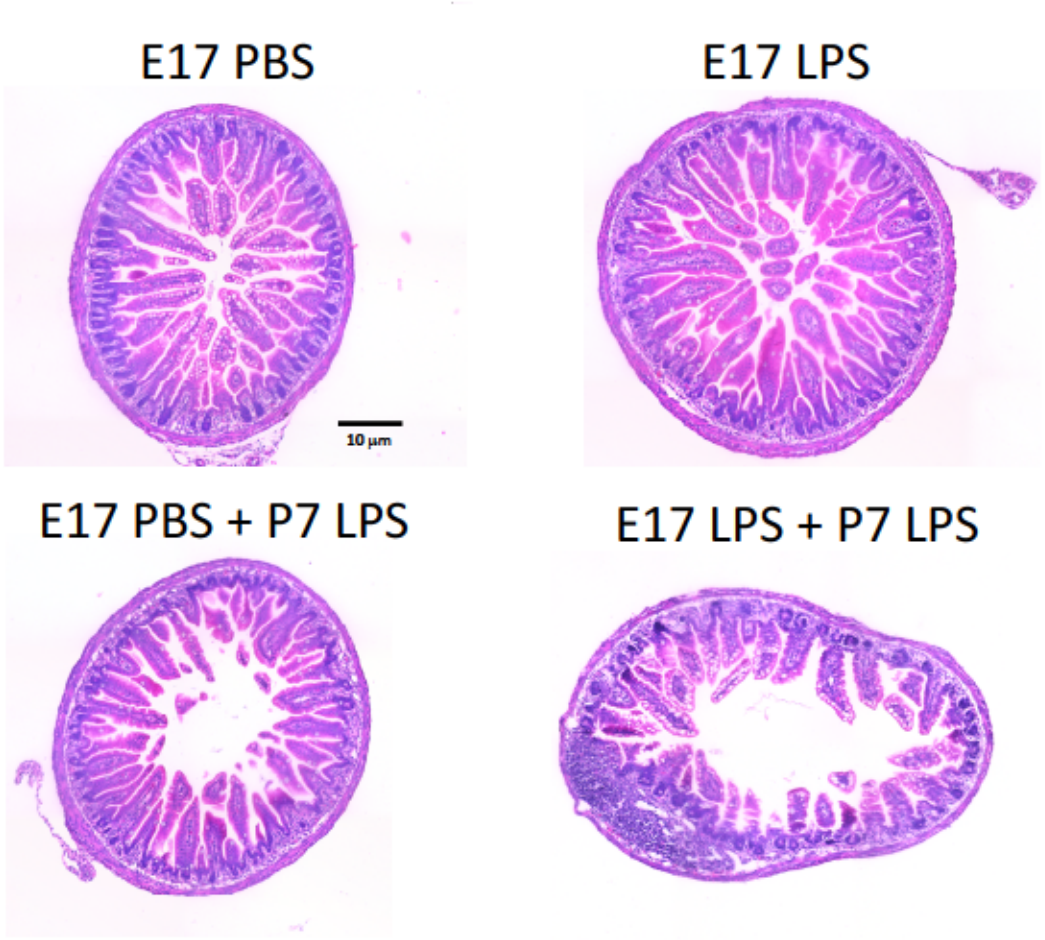

Figure 3.6. ***Endotoxin tolerance effects in the ileum due to prenatal LPS exposure largely disappear after ten days of life.*** qRT-PCR measurements from ileums of mice that were exposed to either LPS (2 mg/kg) or PBS at E17 and then LPS again at postnatal day 10 (P10). Each gene is indicated above the graph, each point represents an individual mouse, and all expression levels are relative to RPL0 expression. $n \geq 4$ animals analyzed per group. All data is representative of three separate experiments and one-way ANOVA tests were performed to determine significance.

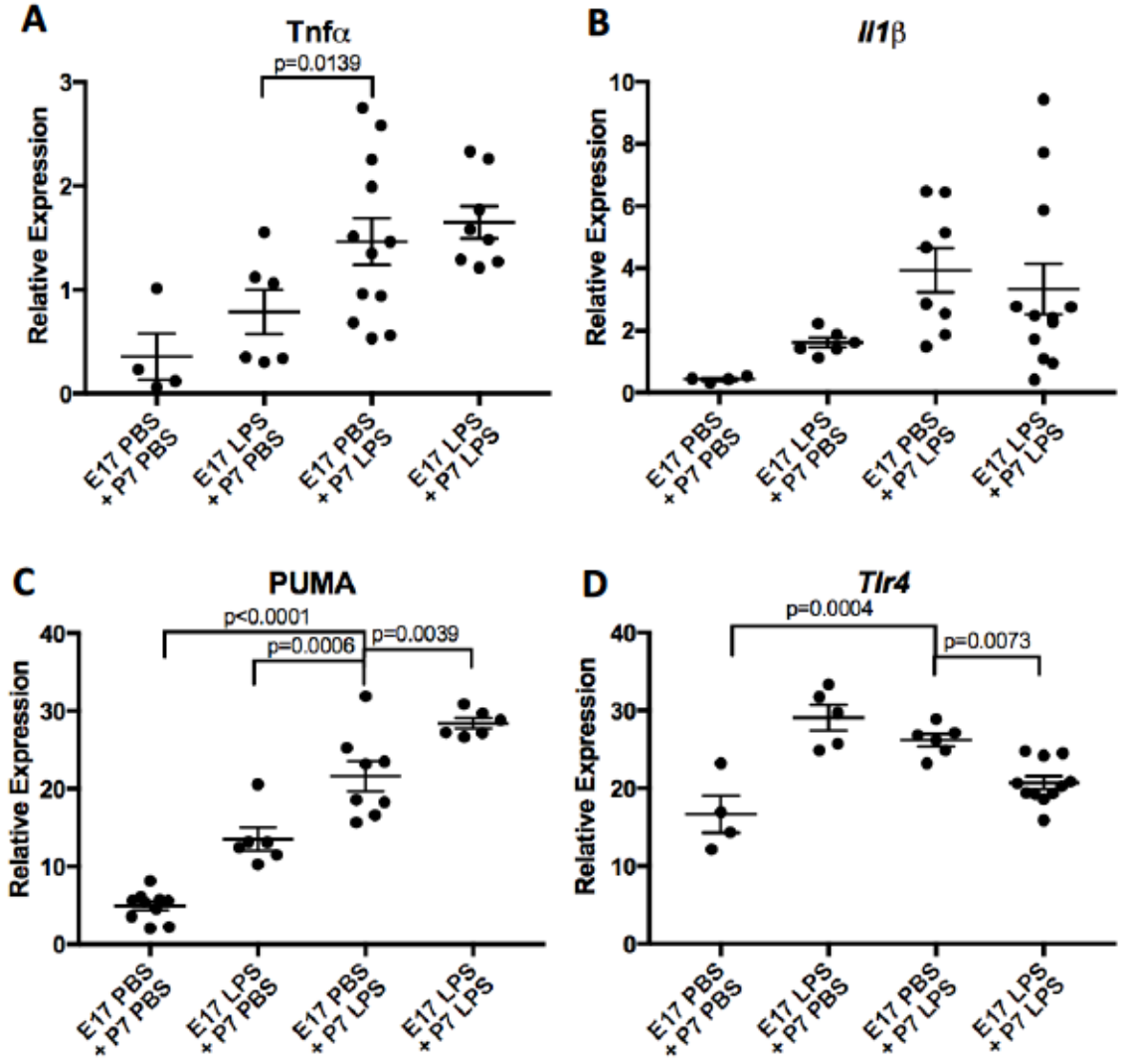

Figure 3.7. ***Prenatal LPS exposure does not protect ileum integrity after postnatal day 10 LPS exposure.*** **(A)** Representative micrograph of H & E staining in the ileum of mice that were exposed to either LPS (2mg/kg) or PBS at E17 and LPS at postnatal day 10 (P10). All data is representative of three separate experiments ($n \geq 4$ per group, per experiment).

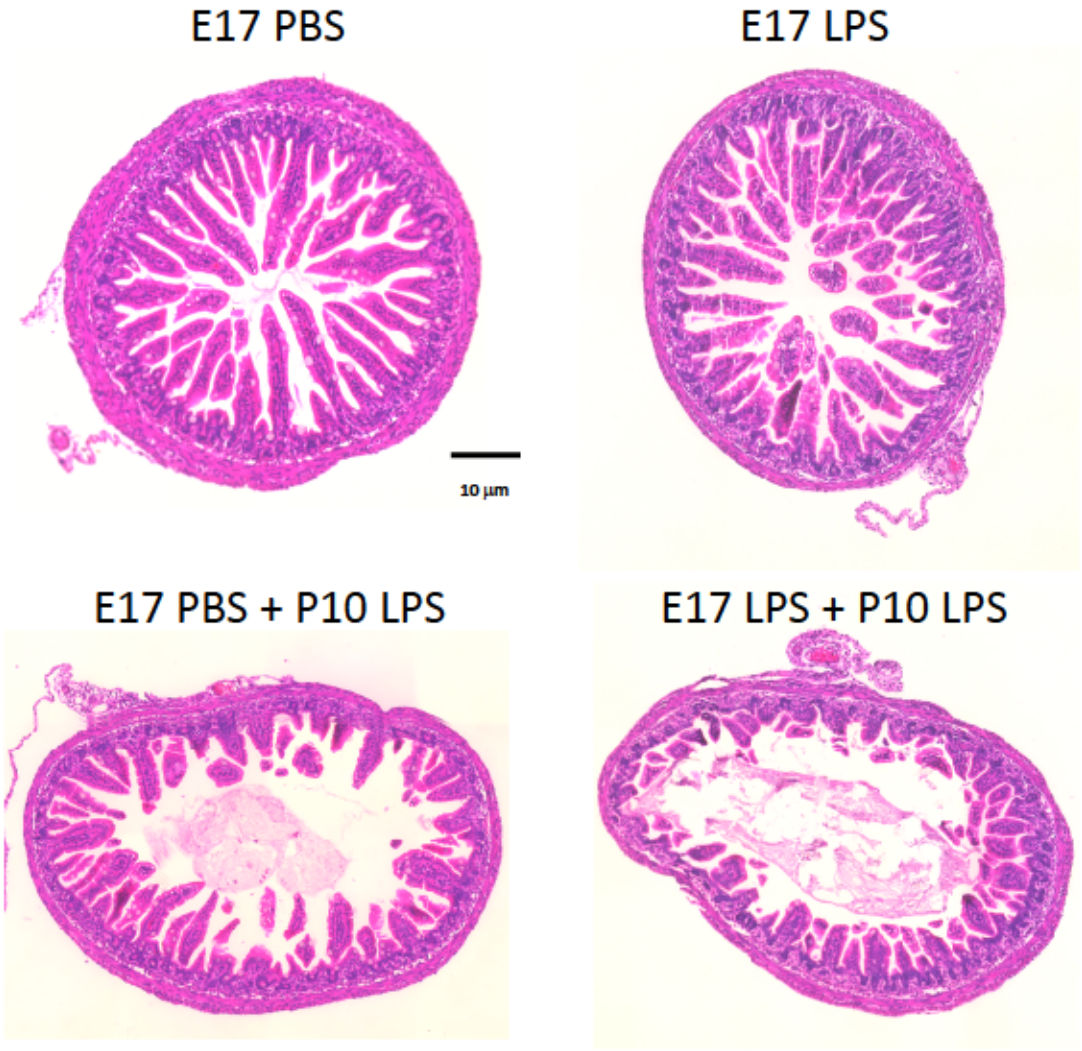

Table 3.1. Primers used for *in utero* plus early postnatal endotoxin exposure qRT-PCR experiments.

Primer	Species	Forward Sequence	Reverse Sequence	Amplicon Size (bp)
RPL0	Mouse/Rat/Human	GGCGACCTGGAAGTCCAACT	CCATCAGCACCACAGCCTTC	143
IL1β	Mouse/Rat	AGTGTGGATCCCAAGCAATACCCA	TGTCCTGACCACTGTTGTTTCCCA	175
TNFα	Mouse/Rat	TTCCGAATTCACTGGAGCCTCGAA	TGCACCTCAGGGAAGAATCTGGAA	144
Tlr4	Mouse	TTTATTCAGAGCCGTTGGTG	CAGAGGATTGTCCTCCCATT	186
PUMA	Mouse/Rat	GCAGTACGAGCGGCGGAGAC	GGGCGGGTGTAGGCACCTAGT	149

Discussion

These findings both support and contradict our initial hypothesis that *in utero* exposure to LPS protects against postnatal inflammation. Specifically, we have shown that mice exposed *in utero* at E17 to LPS develop endotoxin tolerance within the ileum and do not mount a typical immune response upon exposure to LPS postnatally at day 1 of life. Expression of inflammatory markers were all significantly reduced compared to mice exposed to E17 PBS plus P1 LPS. Cell proliferation among E17 LPS plus P1 LPS exposed mice was significantly increased, though this did not translate to noticeable histological differences across groups. However, these results did not persist when E17 LPS exposed mice were exposed to postnatal LPS at varying time points. Among mice exposed to LPS at P7 instead of P1, there was no significant difference expression of in most inflammatory markers between E17 PBS plus P7 LPS exposed mice and E17 LPS plus P7 LPS exposed mice. Consistent with these results, P7 LPS exposure among both E17 PBS and LPS groups showed a visible breakdown in ileum tissue and villi structure upon H & E staining. In a final set of experiments, LPS exposure occurred at P10 after initial E17 exposure to either PBS or LPS. These experiments verified that the state of endotoxin tolerance among E17 LPS exposed mice was limited to the first days of life and no longer present by P10, as there was no significant difference in proinflammatory cytokine expression and an increase in apoptosis among E17 LPS plus P10 LPS exposed mice. The latter finding was confirmed upon histological staining, which clearly showed a breakdown in tissue structure and villi integrity among all mice exposed to P10 LPS, regardless of E17 exposure status.

Endotoxin tolerance has been shown to be a state of reduced endotoxin-associated mortality after an initial sub-lethal dose of LPS. This state of tolerance is often temporary, with peak hypo-responsiveness occurring a few days after the initial LPS exposure and typical immune function occurring within eight days [38]. In the healthy intestine, exposure to a high dose of LPS causes a significant increase in the innate immune response in early life, potentially leading to tissue damage and death. Specifically, levels of cytokines like TNFα and *IL1β* spike after exposure as they are often the downstream signals of genes critical for normal immune function, like *Tlr4*. In concert, these signals trigger pain and subsequent inflammation. Conversely, in endotoxin tolerance, pro-inflammatory cytokine levels do not increase, instead mimicking immune function of those not exposed to LPS, nor do innate immunity genes [38,40]. A muted immune response early in life may, upon first glance, appear to be entirely beneficial, protecting the vulnerable neonate from developing septic shock. However, these patients develop an increased risk of secondary infection during an already vulnerable period of development.

Taken together, these results suggest a temporary but significant effect of *in utero* exposure on the postnatal intestinal immune system. Though the causal mechanism of this protective effect remains unknown, the approach used in this study can contribute to work regarding both endotoxin tolerance and its associated mechanisms (e.g. microRNAs). By conducting these important preliminary experiments, it is hoped that further work will be done to discern the causal mechanism behind the muted immune response associated with a second exposure to bacteria, with mechanistic knowledge allowing for development of therapeutic approaches for neonatal sepsis patients.

Chapter 4

Prenatal endotoxin exposure does not determine necrotizing enterocolitis severity in mice

Methods

Mouse model of necrotizing enterocolitis

Though important biological information can be gleaned from the above experiments, we saw the importance of putting any potential findings into a disease context and thus chose to study an early life model for NEC, a leading cause of gastrointestinal-related disease in newborns that is often associated with prematurity (see **Chapter 1**). After intrauterine injection of LPS or PBS (2 mg/kg) at E17, mice were birthed naturally and housed with their mother until the model began. NEC was induced in mouse pups by the administration of gavage-fed formula every three hours and exposure to hypoxic conditions twice per day from P7-P10 (**Figure 4.1**). Breast fed, age-matched pups were used as controls as previous studies have shown that tissue from breast fed pups is indistinguishable from that of control pups that received gavage-fed formula upon analysis via qPCR and immunostaining. The mice were then euthanized at P11 and ileum samples were collected and placed in 4% paraformaldehyde (Electron Microscope Services, Cat #RT15700) in PBS overnight or flash-frozen in liquid nitrogen and stored at -80 degrees Celsius for later use.

Quantitative real-time PCR and histology staining

The methods for qRT-PCR outlined in **Chapter 3** were used in these experiments, as were the primers outlined in **Table 3.1**. We also performed Alcian blue staining on ileum tissue from both exposure groups. Briefly, the paraffin-embedded ileum samples were probed with Alcian blue (Sigma-Aldrich) for half an hour and nuclear fast red (Sigma-Aldrich) for one hour at room temperature then washed and mounted using Permount mounting media (Fisher Scientific, see **Chapter 3** for additional methods).

Statistical analysis

Data were analyzed using GraphPad Prism 7 software. All data were analyzed for significance using a one-way ANOVA test and post hoc Bonferroni correction for multiple comparisons. Statistical significance was determined by a p-value of <0.05. All PCR was performed in triplicate, with at least five pups in each experimental group. Data was assembled and graphed using GraphPad Prism 7.

Prenatal LPS exposure does not cause a significant change in immune response to NEC in the ileum

To determine whether *in utero* LPS exposure has an effect on NEC severity, we evaluated pro-inflammatory cytokine expression in the ileum using qRT-PCR. These results showed that there was no significant difference in expression of the cytokines Tnfα and *IL1β* (**Figure 4.2A-B**) and both cytokines were expressed at levels similar to previously published NEC models [52]. Quantification of PUMA expression showed that both groups had high levels of apoptosis after undergoing the NEC model (**Figure 4.2C**).

We then assessed expression of *Tlr4*, whose exaggerated expression is a crucial part of the pathogenesis of NEC. In **Figure 4.2D**, we saw elevated expression levels consistent with the literature but no significant difference between the E17 LPS and E17 PBS exposed groups after they went through the NEC model [48,53,54].

No histological evidence of a difference in NEC severity between E17 LPS and E17 PBS groups

To further determine whether there was a significant difference in NEC severity between both exposure groups, we performed Alcian blue staining on ileum samples from both groups. Our results showed a breakdown in villi structure and organization within the ileum in both groups, indicating reduced barrier function and absorption as well as increased inflammation (**Figure 4.3A-B**). These results are consistent with published results on the tissue damage associated with NEC [53,54].

>*8?&.!IA@AA*Illustrated depiction of the intrauterine injection plus four day necrotizing enterocolitis (NEC) exposure experimental model.* C*1&0&/1#=&,7# 9/3%&++&*(#03*%#P7-2&31#B#DEQRJ

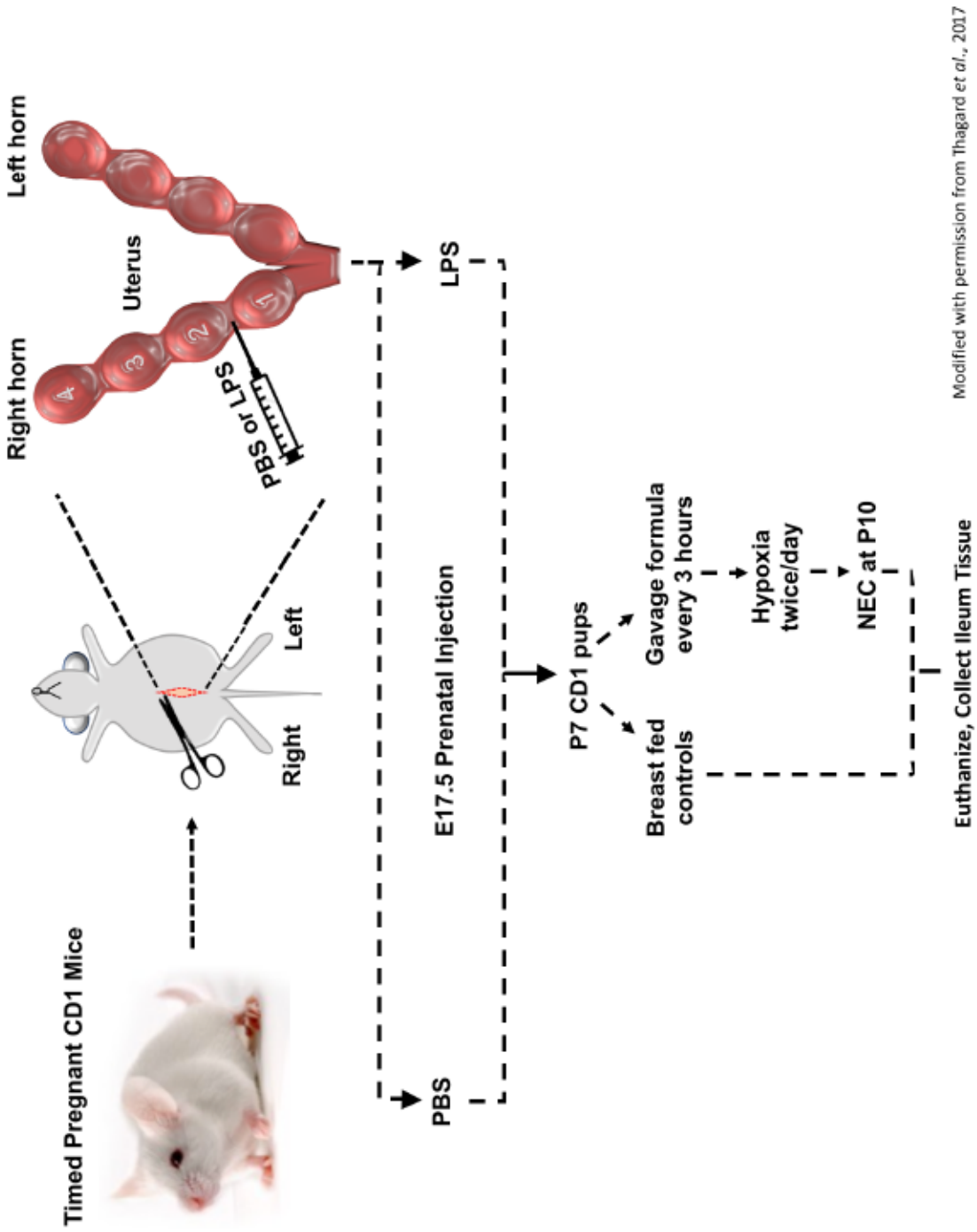

#

'*

Figure 4.2. ***Prenatal LPS exposure has no effect on the immune response associated with necrotizing enterocolitis.*** qRT-PCR measurements from ileums of mice that were exposed to either LPS (2 mg/kg) or PBS at E17 and then a four day NEC model. Each gene is indicated above the graph, each point represents an individual mouse, and all expression levels are relative to RPL0 expression. $n \geq 11$ animals analyzed per group. All data is representative of two separate experiments and one-way ANOVA tests were performed to determine significance.

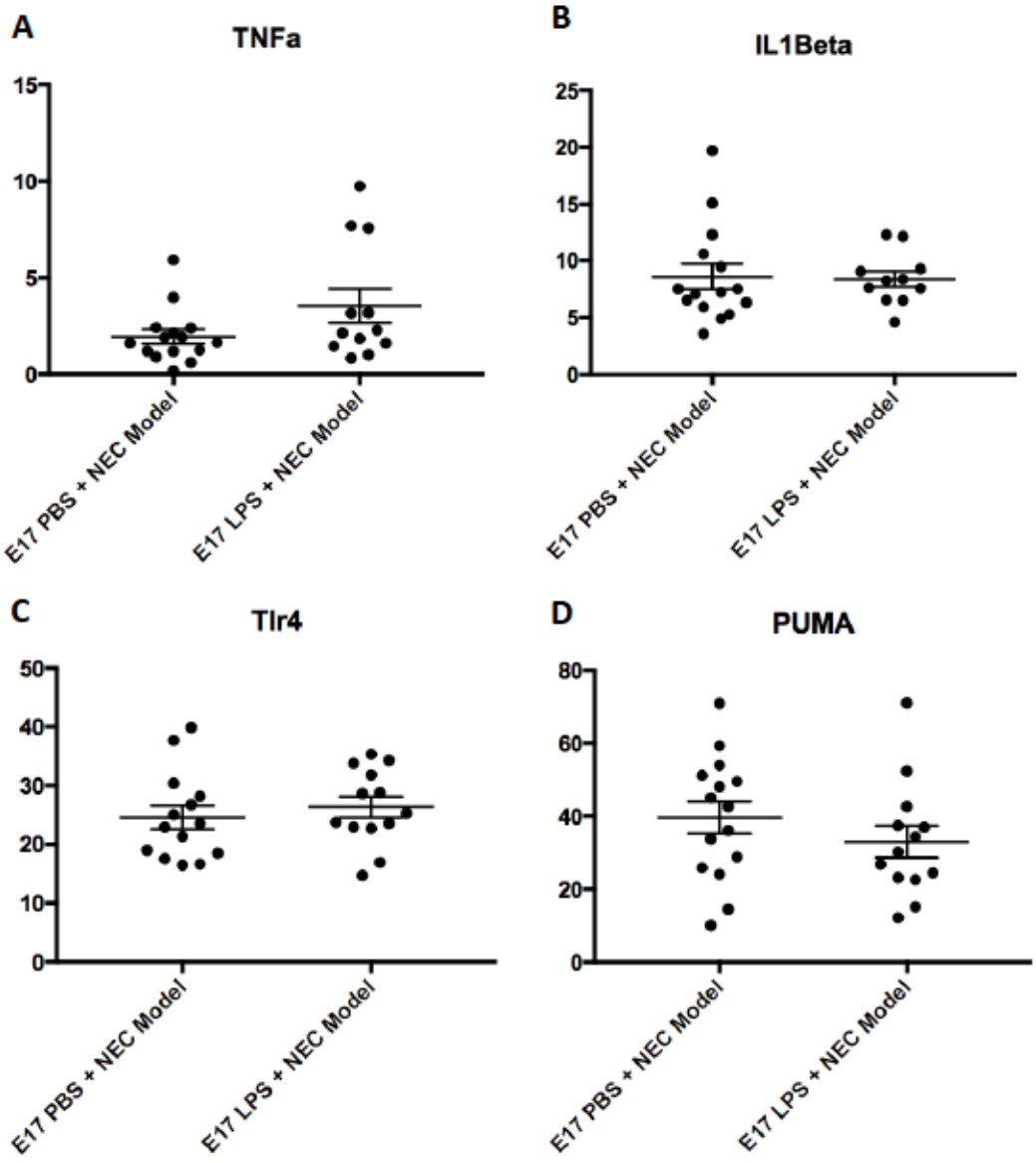

Figure 4.3. ***Prenatal LPS exposure does not protect against tissue degradation associated with necrotizing enterocolitis.*** Representative Alcian blue staining of ileums that were exposed LPS (2 mg/kg) or PBS at E17 and subsequently exposed to a four day NEC model.

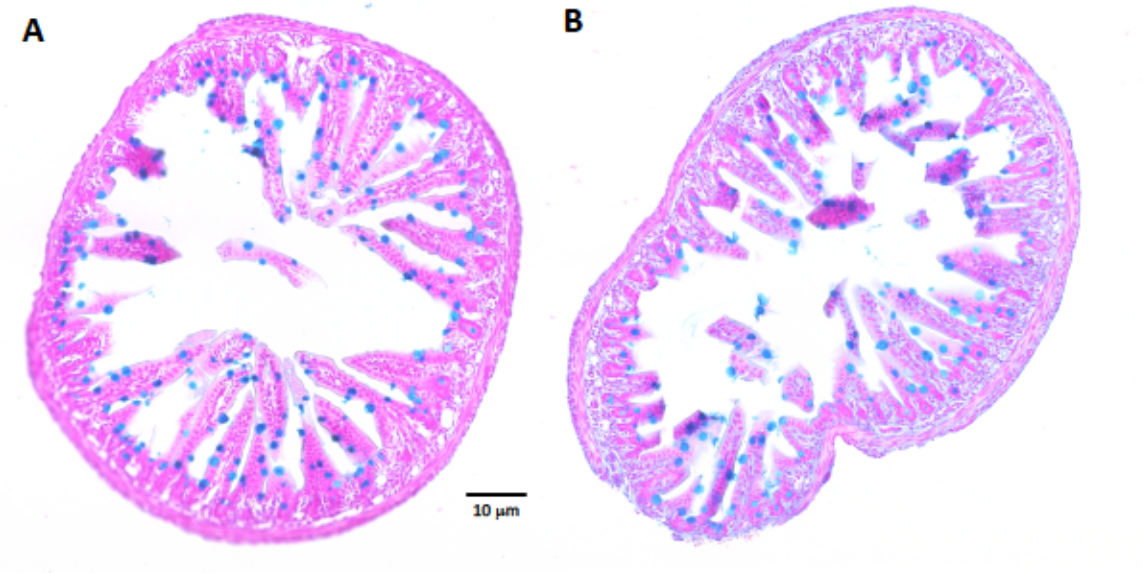

Discussion

The current findings do not support our hypothesis that *in utero* exposure to LPS will reduce NEC severity after completion of a four day NEC model. Instead, we found that there was no significant difference in proinflammatory cytokine production, apoptosis, or *Tlr4* expression and that all markers indicated disease in both the E17 LPS and E17 PBS exposed mice exposed to the NEC model. Histologic analysis also revealed tissue damage consistent with published results in human, piglet, and mouse NEC [53]. Taken together, these findings indicate that *in utero* exposure to LPS does not have a significant effect on NEC development. Though our study attempted to explain the seemingly random incidence of NEC across populations of premature neonates, it appears that the critical window for disease development is not during the late stages of *in utero* development.

Chapter 5

Prenatal endotoxin exposure is protective against DSS colitis

Methods

Dextran sulfate sodium-induced colitis model in the mouse

All mice, regardless of the LPS or saline exposure they received at E17 or P7, underwent a six day DSS model (**Figure 5.1**) as follows: On day 1 of the model, the mice were weighed and given either 2% DSS (MW 40,000-50,000 kDa, Thermo Scientific) in 0.5% sucrose drinking water; control mice received 0.5% sucrose drinking water alone. Mice were weighed each day of the model and on day three, fresh 2% DSS/0.5% sucrose or 0.5% sucrose water was offered. On day six, all mice were offered regular water and euthanized on day seven. Before euthanization, colonoscopy (see below) was performed using isoflurane anesthesia administered via nose cone. Colon length was measured, and then flash-frozen in liquid nitrogen and stored at -80 °C. Cages were separated by sex and exposure throughout the model.

Mouse colonoscopy

Colonoscopy was performed on six-week-old mice upon conclusion of the six day 2% DSS model before euthanization. Isoflurane anesthesia was administered via a nose cone. Colonoscopy was then performed using a Karl Storz endoscope (Cat #61029D) with an attached air syringe. The endoscope was coated with surgical lubricant

(Puralube) and inserted into the anus. Air was slowly pushed from the syringe to allow a field of view and pictures were taken using a StarTech HDMI Video Capture device. Mice were euthanized after the procedure was completed.

Quantitative real-time PCR transcriptomic analysis

RNA was extracted from colon tissue and quantitative real-time PCR was performed using methods outlined in **Chapter 3. Table 5.1** shows all primers used in these experiments and expression was relative to the housekeeping gene ribosomal protein large P0 (RPL0).

Immunofluorescence and histology

For Alcian blue staining, the collection, fixation, and section cutting processes outlined in **Chapter 3** were used. The paraffin-embedded samples were probed with Alcian blue (Sigma-Aldrich) for half an hour and nuclear fast red (Sigma-Aldrich) for one hour at room temperature then washed and mounted in Permount mounting media (Fischer Scientific). For ZO-1 tight junction staining, paraffin-embedded colon samples were prepared using the methods outlined in **Chapter 3** and then stained with 4',6-diamidino-2-phenylindole (DAPI), anti-ZO-1 (ThermoFisher, Cat# 61-7300), and Alexa Fluor 555 donkey anti-mouse at 1:1000 for two hours at RT then washed and mounted in Gelvatol mounting media.

Microscopy and fluorescence quantification

All Alcian blue images were acquired using a Leica DMi8 inverted microscope. Images were captured using a 20X objective (Leica HC PLAN 20X/0.70). The images were analyzed using Fiji and quantified using Excel. Five unique mucosal thickness measurements were recorded for each sample and the average was calculated. All immunofluorescence images were acquired using methods outlined in **Chapter 3**.

16S rRNA sequencing of bacteria in mouse stool

Stool from mice that underwent *in utero* injection of PBS or LPS and subsequent 2% DSS exposure or 0.5% sucrose control exposure was isolated from the colon at euthanasia by extraction from the tissue with forceps and flash-frozen using liquid nitrogen then stored at -80 °C. Bacterial genomic DNA was isolated using a DNeasy PowerSoil Kit (Cat #12888-50, Qiagen), and processed at the Johns Hopkins Transcriptomics and Deep Sequencing Core for library preparation and 16S rRNA sequencing (MiSeq 2x150, V3V4 sequencing). Quality trimming (target error rate <0.5%), PhiX removal, chimera detection, host genome removal, and unknown contaminant assessment for non-16S sequences were performed. Data were normalized to 10,000 high-quality 16S rRNA sequences. High-resolution taxonomic assignment was performed by Resphera Insight (Baltimore, Maryland, United States), functional inference of gene content was found using PICRUSt, alpha and beta-diversity calculations were made using QIIME, and principal coordinates, differential abundance of alpha diversity, and taxonomic categories analyses were performed using R.

Statistical analysis

Data were analyzed using GraphPad Prism 7 software. All data were analyzed for significance using a two-tailed t-t test or one-way ANOVA and post hoc Bonferroni correction for multiple comparisons. Statistical significance was determined by a p-value of <0.05. All PCR was performed in triplicate, with at least five pups in each experimental group. Data was assembled and graphed using GraphPad Prism 7.

Prenatal LPS exposure protects mice from subsequent development of experimental colitis in adulthood

To determine the effects of prenatal endotoxin exposure on colitis severity in adulthood, we analyzed colon tissue from six-week old CD-1 mice that had been exposed *in utero* to either LPS (2 mg/kg) or PBS, and which were subsequently exposed to a 6 day DSS-colitis model. Colonoscopy was performed on the 6-week-old mice while they were under general anesthesia in order to initially assess the severity of colonic inflammation. As shown in **Figure 5.2**, we observed significant inflammation and bleeding in the colon in mice that had received PBS at E17 and subsequently exposed to DSS colitis which was characterized by mucosal friability and edema. Strikingly, the *in utero* exposure at E17 to LPS significantly reduced the degree of inflammation, and the colonic mucosa appeared to resemble untreated mice. Colonoscopies were also performed in mice that were induced to develop colitis after prior exposure to either LPS or PBS on day seven of life. Both of these DSS-exposed groups displayed significant inflammation and bleeding within the colon, while control mice not exposed to DSS did not (**Figure 5.2**).

Prenatal exposure to LPS reduces the effects of colitis on weight loss and colon length

To further assess the effects of the *in utero* exposure to LPS on the physiologic manifestations of subsequent colitis development, we assessed the degree of weight loss and colonic shortening, both established markers of colitis severity [55,56]. Mice were weighed on each day of the 6-day model across all experiments, and their weight change over the six days is displayed in **Figure 5.3A-D**. Sex did not have an effect on colitis severity, as revealed by a lack of significant difference between male and female mice within each exposure group across experiments, after adjusting for initial weight differences between sexes (**Figure 5.3A-D**). Mice injected with PBS *in utero* that were not exposed to DSS at five weeks did not lose weight over the six days corresponding to the DSS model duration (mean weight gain= 2.1 g ± 0.9) as expected (**Figure 5.3A**). There was also no weight loss in mice injected with LPS at E17 that were not exposed to DSS at five weeks (mean weight gain=2.0 g ± 0.3), confirming that the initial LPS injection did not have major independent effects on growth (**Figure 5.3B**). Importantly, mice that were exposed to PBS at E17 and then subsequently to DSS at five weeks showed significant weight loss, losing an average of 0.6 ± 0.4g over the six day model (**Figure 5.3A**). Strikingly, mice that were exposed to LPS in utero at E17 and then induced to develop colitis at five weeks showed significantly less weight loss than these control groups (mean weight gain=1.6 g ± 0.2, **Figure 5.3B**). These findings reveal that *in utero* LPS exposure protects against the weight loss that is associated with DSS colitis, and instead actually gained weight during the model.

Further validation of the protective effects of *in utero* exposure to LPS on the subsequent development of colitis is shown in **Figure 5.4A-C**, in which colon length measurements are shown and which stratified by sex. Consistent with measures of weight change, colon length was not significantly different between male and female mice within each exposure group. Unlike control mice which had average colon lengths between 9.1-9.9 cm, mice who were exposed to colitis after *in utero* exposure to PBS revealed a significantly shorter average colon length of 7.6 cm (**Figures 5.4A** and **5.4C**), a finding consistent with the development of colonic inflammation. By contrast, the exposure *in utero* to LPS markedly reduced the degree of colonic length shortening when they were subsequently induced to develop colitis, and the lengths were between 9.1-9.9 cm, similar to control mice (**Figure 5.4B-C**). These results support the notion that the in utero exposure to LPS significantly protects mice from colon shortening associated with the onset of experimental colitis.

It was critical for us to define whether the observed protective effects of LPS were attributable to exposure in the *in utero* environment or whether the protective effects of LPS occurred independent of the window of exposure, suggesting some degree of endotoxin tolerance. To test for this possibility, we next repeated the above experiments by exposing mice to PBS or LPS (2 mg/kg) at postnatal day 7 without prior *in utero* exposure. As shown in **Figures 5.3 C-D** and **5.5A-C**, in contrast to the protective effect of *in utero* LPS injection, mice that received PBS or LPS at 7 days of age followed by the induction of DSS colitis at five weeks experienced no protection from LPS exposure. Specifically, mice receiving LPS at 7 days revealed significant weight loss over the six day DSS colitis model (**Figure 5.3D**), which did not differ across sexes, and was similar

to the colitis-induced weight loss that mice receiving PBS at 7 days (**Figure 5.3C**). Additionally, mice that received LPS at day 7 and subsequently developed colitis revealed significantly shorter colon lengths than relevant controls and displayed no protection from LPS pre-exposure (**Figure 5.5B-C**), unlike the mice who received LPS at E1 but similar to mice who received PBS at 7 days (**Figure 5.5A**).Taken together, these results indicate that *in utero* exposure of LPS at E17 significantly protects against the subsequent development of colitis, and that the protection is not seen when LPS is given at later time-points postnatally. We next sought to determine the mechanisms involved, and evaluated first the inflammatory gene expression in epithelial cells between groups.

Prenatal LPS exposure leads to reduced inflammation and increased Muc2 expression in the adult mouse colon

In seeking to determine the mechanisms of *in utero* LPS exposure to subsequent colitis development, we next evaluated whether *in utero* exposure to LPS could alter the degree of mucosal pro-inflammatory cytokine expression. As shown in **Figure 5.6A-C**, there was a significant increase in expression of the pro-inflammatory cytokines *IL1β*, Tnfα, and IL-6 within the colons of mice that were exposed to DSS after prior *in utero* exposure to PBS at E17, and the degree of expression was higher than all other groups. Expression of the tight junction gene *Cldn1* was not significantly different across groups (**Figure 5.6D**). By contrast, expression of the mucus producing goblet cell gene *Muc2* was significantly increased in the colitis mice that had received LPS at E17(**Figure 5.6E**), consistent with a role for *in utero* LPS on restoration of the intestinal epithelial barrier. Importantly, the induction of colitis in mice that received saline at E17 resulted in

significant upregulation of the expression of the LPS receptor gene *Tlr4*. Strikingly, mice that received LPS *in utero* at E17 showed significantly reduced expression of *TLR4* upon the subsequent induction of colitis (**Figure 5.6F**). As expected, mice that were not exposed to colitis did not reveal any significant increase in *Tlr4* (**Figure 5.6F**). Of note, control mice with colitis that had been exposed to LPS or PBS at day 7 of life of *in utero* at E17 showed no differences in the expression for *IL1β* and IL-6 (**Figure 5.7B-C**). We did observe a persistent increase in Tnfα expression in mice with colitis that received PBS at P7 as compared to mice that received LPS at P7 (**Figure 5.7A**). There were no significant expression changes across the IBD-associated genes analyzed in this study in mice that were exposed to PBS or LPS at day 7, including *Cldn1, Muc2,* and *Tlr4* (**Figure 5.7D-F**) Overall, these findings reveal that exposure to LPS *in utero* leads to reduced inflammation and increased *Muc2* expression in mice with colitis, while such protection was not observed in mice that were treated with LPS or PBS at P7. To further investigate the mechanisms mediating this effect, we next evaluated whether epithelial cell barrier function was affected by *in utero* exposure to LPS.

Prenatal LPS exposure minimizes the loss of goblet cells and tight junctions in adult mice with experimental colitis

An important potential pathway by which LPS exposure *in utero* could protect against the subsequent development of colitis lies in the protective mucosal layer of the colonic epithelium, which is developmentally regulated through the *Math1* pathway, and which we have shown to be influenced by activation of TLR4 developmentally [57]. We therefore next whether *in utero* exposure to LPS could alter the degree of mucin-

producing cells within the gut. As shown in **Figure 5.8A**, the induction of colitis led to a striking loss of goblet cells in the intestinal epithelium in mice exposed to PBS *in utero*. This loss of goblet cells was not observed in mice exposed to LPS *in utero*, again reflective of *in utero* protection by LPS. To quantify the extent of mucus production, mucosal layer thickness was measured for each sample, as a validated readout of mucin production in the DSS model [55]. As shown in **Figure 5.8B** the mucosal thickness of mice with colitis that had been exposed to LPS *in utero* was similar to control mice that did not receive DSS, confirming that the protection extends towards mucous protection in adulthood. Control mice with colitis that were exposed to PBS at E17 displayed reduced goblet cells (**Figure 5.8A**) and a significantly reduced mucosal layer on the intestinal epithelium (**Figure 5.8B**) compared to all other exposure groups, as expected. Further evidence that *in utero* administration of LPS prevented epithelial layer injury was determined by evaluation of tight junction staining via ZO-1 staining. As shown in **Figures 5.9A** and **5.9B**, there was a significant loss of tight junctions in mice with colitis that were injected *in utero* with PBS that was not seen in mice exposed to LPS *in utero*. Importantly, the injection of either LPS or PBS at day 7 did not influence the degree of breakdown in the mucosal barrier thickness as shown in **Figures 5.10A** and **5.10B** and tight junction impairment as compared to the control groups that were not exposed to DSS (**Figure 5.11A-B**). Taken together, these findings reveal that *in utero* LPS exposure limits the loss of the structural barrier in the intestinal epithelium in the setting of subsequent experimental colitis. We next sought to assess whether these results were associated with any microbiotic changes.

Effects of *in utero* exposure to LPS on 16S rRNA sequencing of the microbiome

In the final series of experiments, we assessed whether the *in utero* exposure to LPS altered the stool microbiome during colitis. To do so, we performed 16S rRNA sequencing of stool samples from adult mice that were induced to develop colitis and which had been exposed to LPS in comparison with those that had not. Consistent with the known effects of DSS [58,59], we observed a significant reduction in alpha diversity amongst mice exposed to DSS at five weeks compared to those not exposed to DSS, regardless of their *in utero* exposure (**Figure 5.12B**). This provides support of the notion that that our model is a reliable mimic of human ulcerative colitis and that all mice exposed to DSS at five weeks received an adequate dose of DSS to cause functional change, regardless of whether they displayed any other cellular or inflammatory changes. We also observed a significant increase in *Firmicutes* among E17 PBS exposed mice compared to E17 LPS exposed mice (**Figure 5.12C**). Interestingly, we also observed a significant increase in *Flavobacteria*, a genus within the *Bacteroides* phylum, amongst mice exposed to LPS at E17, regardless of their DSS exposure status (**Figure 5.12D**), consistent with a lasting effect of early LPS exposure. Overall, control mice that did not received DSS exposure had significantly more diverse microbiomes while mice that received E17 PBS had a significantly greater abundance of *Firmicutes* and a significantly reduced abundance of *Flavobacteria* than those that received E17 LPS. These findings suggest an insight into protection as previous work has shown that ulcerative colitis is associated with a reduction in *Firmicutes* bacteria and an increase in *Bacteroides* bacteria, of which *Flavobacteria* belongs [29,60], that persists through adulthood. Taken together, these findings illustrate the importance of *in utero* exposure to LPS in the

protection against subsequent colitis development, and illustrate the long-term effects on barrier injury, gene expression, and the microbiome.

>*8?&.!KA@A ***An illustrated depiction of the intrauterine injection plus 2% DSS exposure experimental model.*** C*1&0&/1#=&,7#9/3%&++&*(#03*%#&?%#BE@RJ

#

)%

Figure 5.2. ***Mouse colonoscopy reveals that prenatal LPS exposure protects mice from subsequent development of experimental colitis in adulthood.*** Representative colonoscopy images from 6 week old mice that either did not undergo a 2% DSS model or underwent a six-day, 2% DSS colitis after earlier exposure to either saline (PBS) or lipopolysaccharide (LPS, 2 mg/kg). LPS or PBS exposure occurred either *in utero* at E17 or on day 7 of life (P7), as indicated. Each colonoscopy image is representative of a single mouse from one of three separate experiments for E17 and P7.

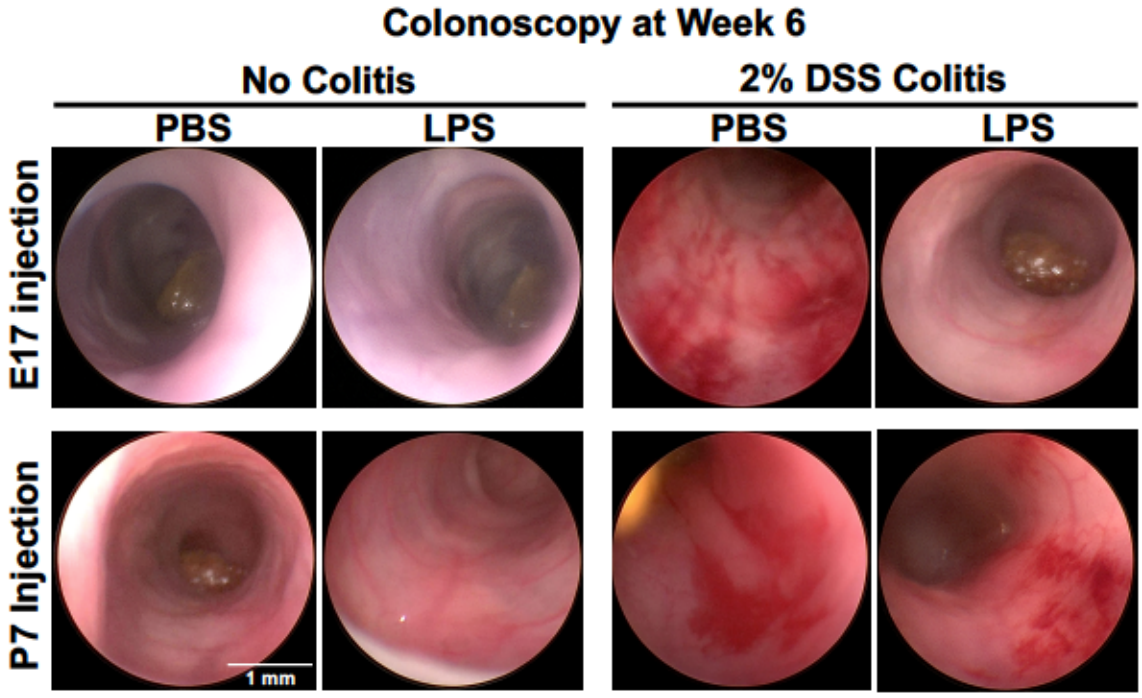

Figure 5.3. ***Prenatal exposure to LPS reduces the effects of colitis on weight loss.*** **(A-B)** Daily weights of 6-week old mice that were injected at E17 with either LPS (2 mg/kg) or PBS. Each point represents group average ($n \geq 5$ for males, $n \geq 3$ for females) weight ± SD. **(C-D)** Daily weights of 6-week old mice that were injected at P7 with either LPS (2 mg/kg) or PBS. Each point represents group average ($n \geq 5$ for males, $n \geq 3$ for females) weight ± SD.

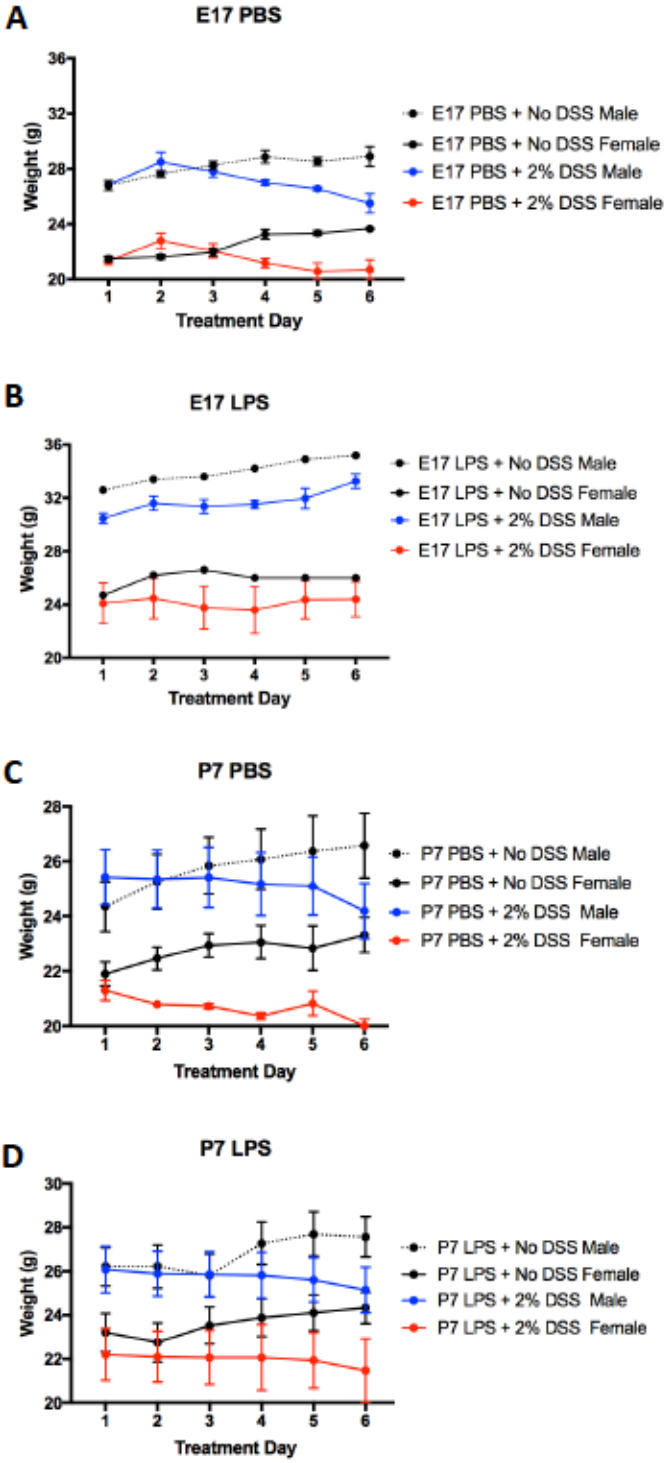

Figure 5.4. ***Prenatal exposure to LPS reduces the effects of colitis on colon length.*** **(A-B)** Colon lengths of 6 week old mice that were injected *in utero* with either LPS (2 mg/kg) or PBS. **(C)** Representative images of colons from each exposure group collected at the end of the DSS model. All data is representative of three separate experiments for E17 exposures and t-tests were performed to determine significance.

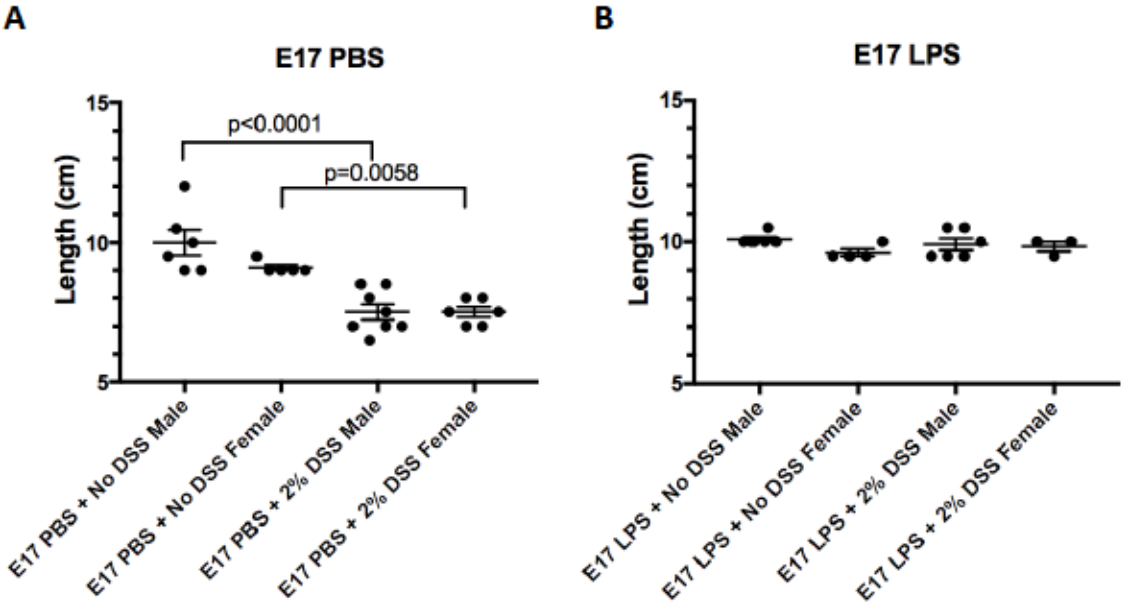

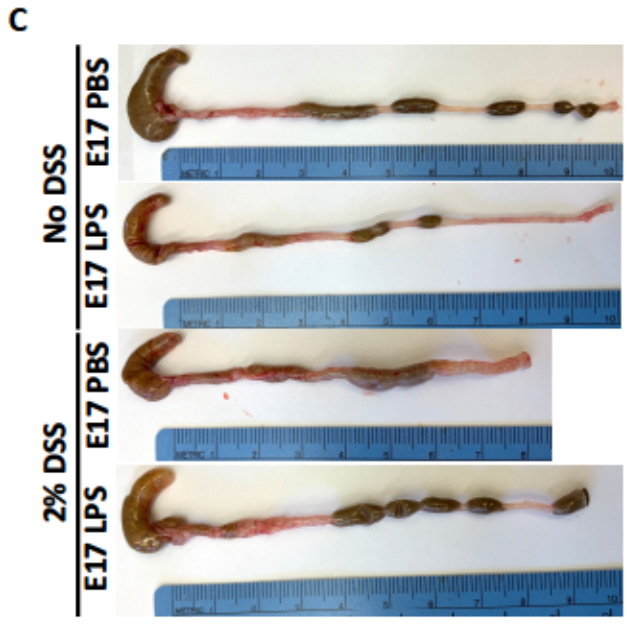

Figure 5.5. ***Postnatal exposure to LPS does not reduce the effects of colitis on colon length.*** (**A-B**) Colon lengths of 6 week old mice that were injected at P7 with either LPS (2 mg/kg) or PBS. (**C**) Representative images of colons from each exposure group collected at the end of the DSS model. All data is representative of three separate experiments for P7 exposures and t-tests were performed to determine significance.

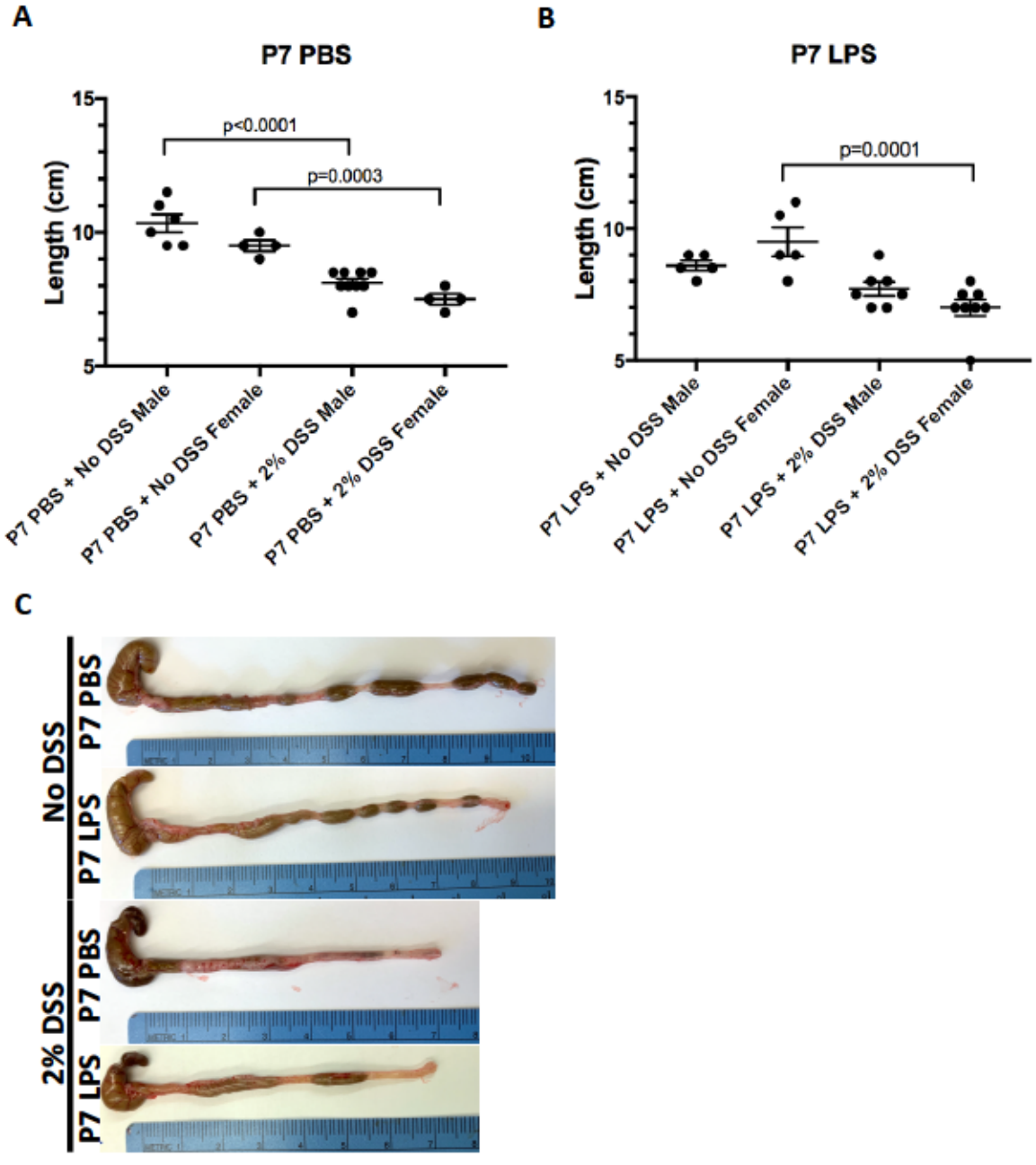

Figure 5.6. ***Prenatal LPS exposure leads to reduced inflammation and increased Muc2 expression in the adult mouse colon.*** qRT-PCR measurements from colons of mice at six weeks of age that were exposed to either LPS (2 mg/kg) or PBS at E17. Each gene is indicated above the graph, each point represents an individual mouse, and all expression levels are relative to RPL0 expression. $n \geq 4$ animals analyzed per group. All data is representative of three separate experiments for E17 exposures and one-way ANOVA tests were performed to determine significance.

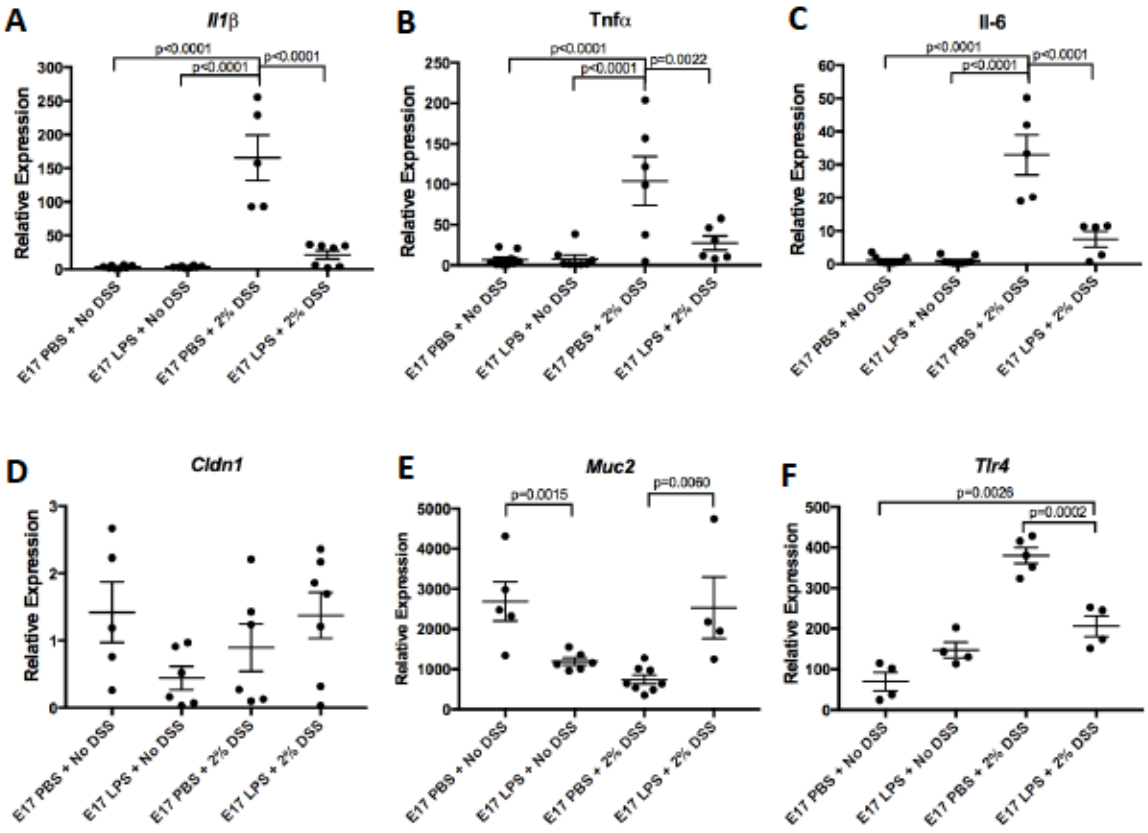

Figure 5.7. ***Postnatal LPS exposure leads to inflammatory response in the adult mouse colon.*** qRT-PCR measurements from colons of mice at six weeks of age that were exposed to either LPS (2 mg/kg) or PBS at P7. Each gene is indicated above the graph, each point represents an individual mouse, and all expression levels are relative to RPL0 expression. $n \geq 5$ animals analyzed per group. All data is representative of three separate experiments for P7 exposures and one-way ANOVA tests were performed to determine significance.

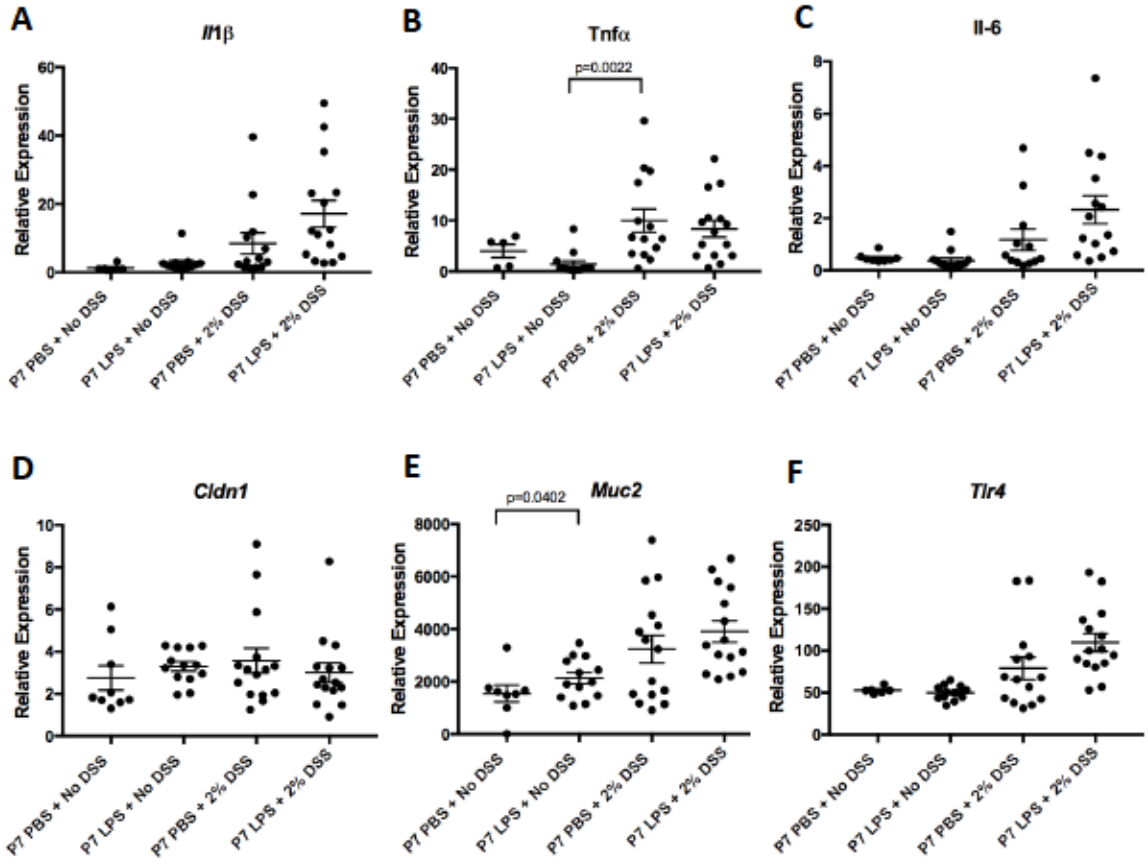

Figure 5.8. ***Prenatal LPS exposure minimizes the loss of goblet cells in adult mice with experimental colitis.*** **(A)** Representative micrograph of Alcian blue staining in the colonic mucosa of 6 week old mice that were exposed to either LPS (2mg/kg) or PBS at E17 and later either not exposed to colitis or exposed to 2% DSS colitis for six days. **(B)** Mucosal thickness quantification measured using the average of five measurements from each sample, as described in Methods. $n \geq 3$ per group. All data is representative of three separate experiments and one-way ANOVA tests were performed to determine significance.

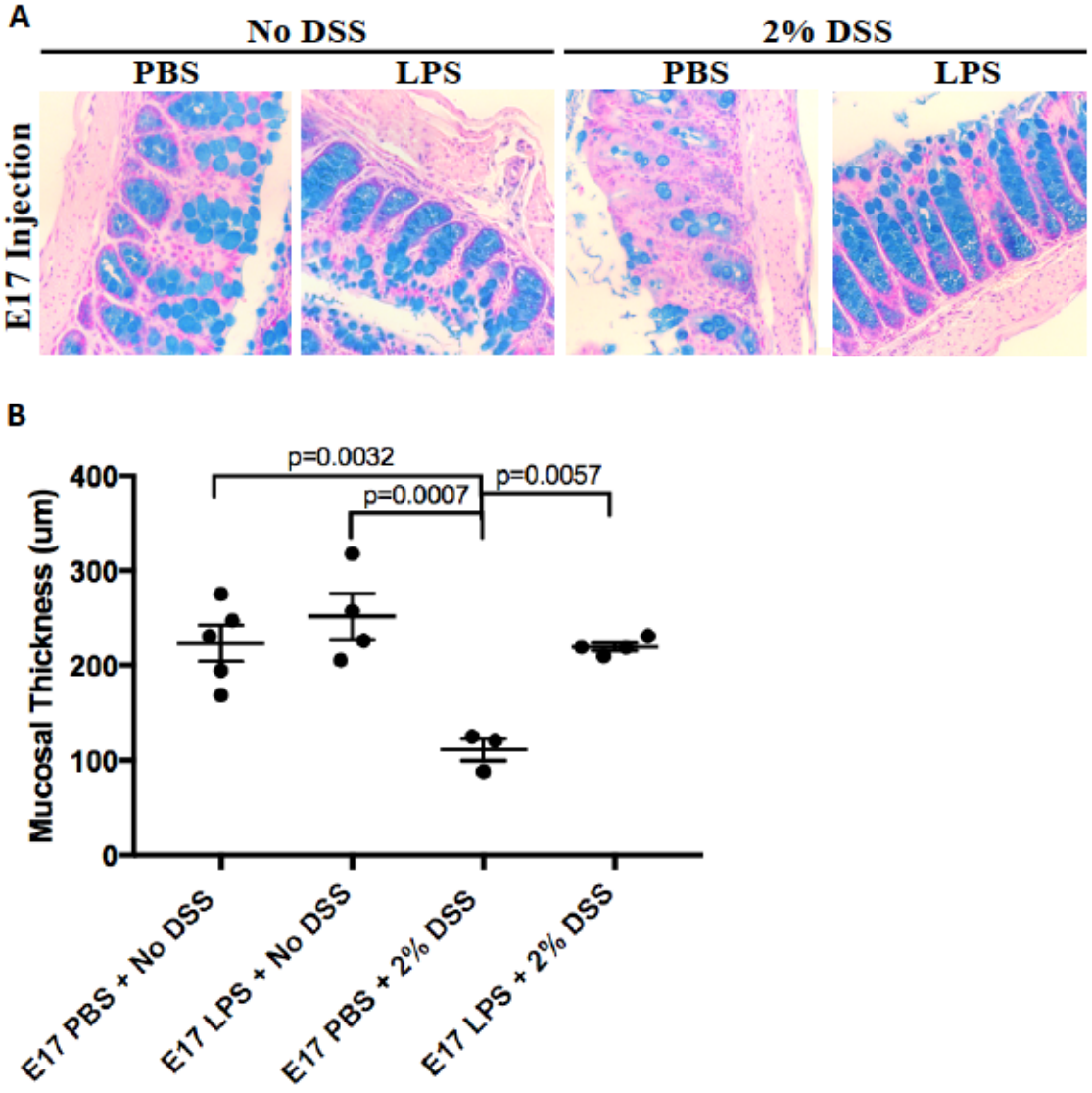

Figure 5.9. ***Prenatal LPS exposure minimizes the loss of tight junctions in adult mice with experimental colitis.*** **(A)** Representative confocal micrographs of the colonic epithelium of 6 week old mice that were exposed LPS (2 mg/kg) or PBS at E17 and subsequently exposed to no colitis or to 2% DSS colitis as indicated. **(B)** Quantification of relative fluorescence measurements of ZO-1 staining compared against DAPI staining. n ≥ 7 per group. All data is representative of three separate experiments and one-way ANOVA tests were performed to determine significance.

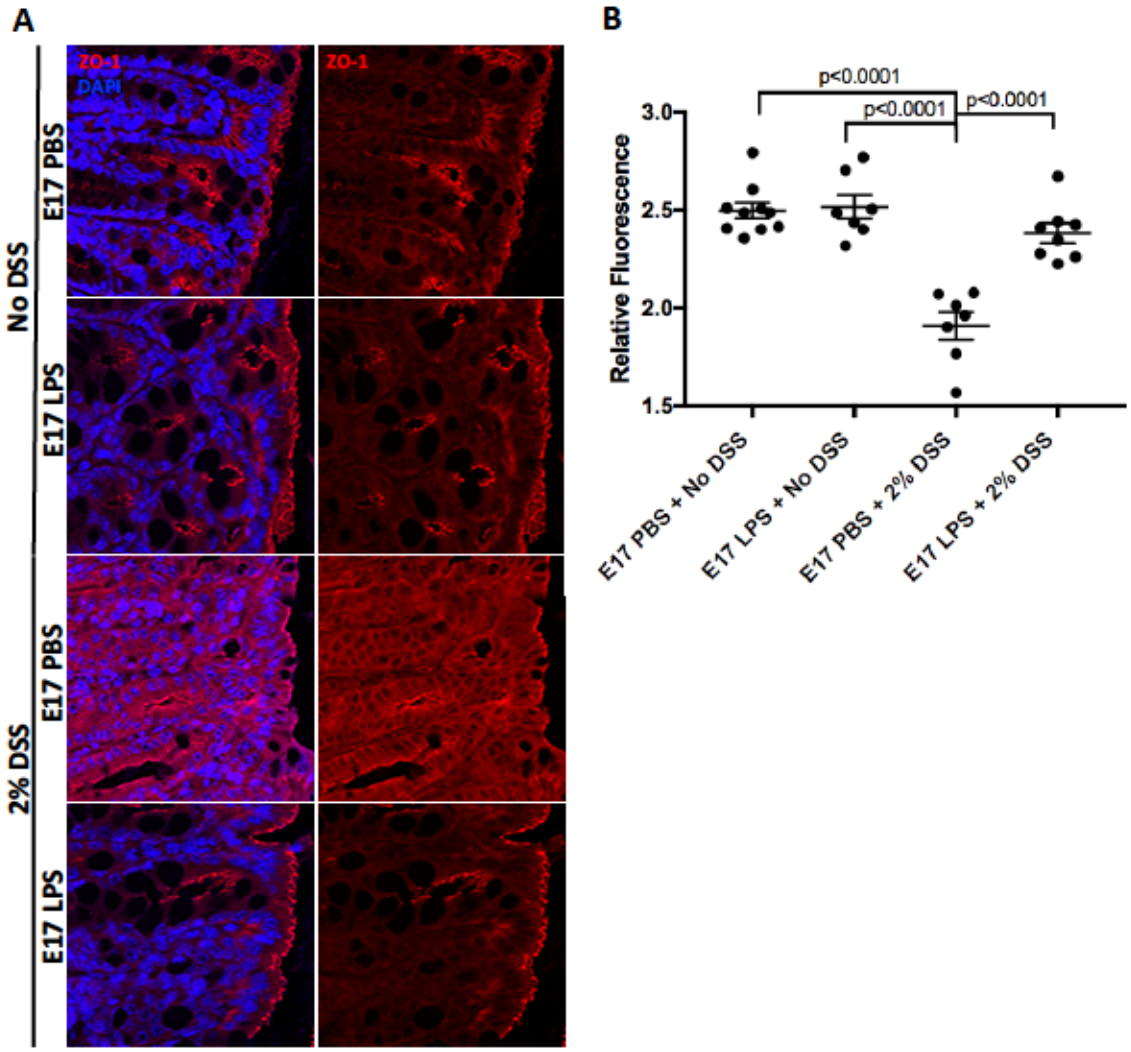

Figure 5.10. ***LPS exposure at day 7 of age does not impact the colitis-induced loss of goblet cells and tight junctions in adult mice.*** **(A)** Representative micrograph of Alcian blue staining in the colonic mucosa of 6 week old mice that were exposed to either LPS (2mg/kg) or PBS at P7 and later either not exposed to colitis or exposed to 2% DSS colitis for six days. **(B)** Mucosal thickness quantification measured using the average of five measurements from each sample, as described in Methods. $N \geq 2$ per group. All data is representative of three separate experiments and one-way ANOVA tests were performed to determine significance.

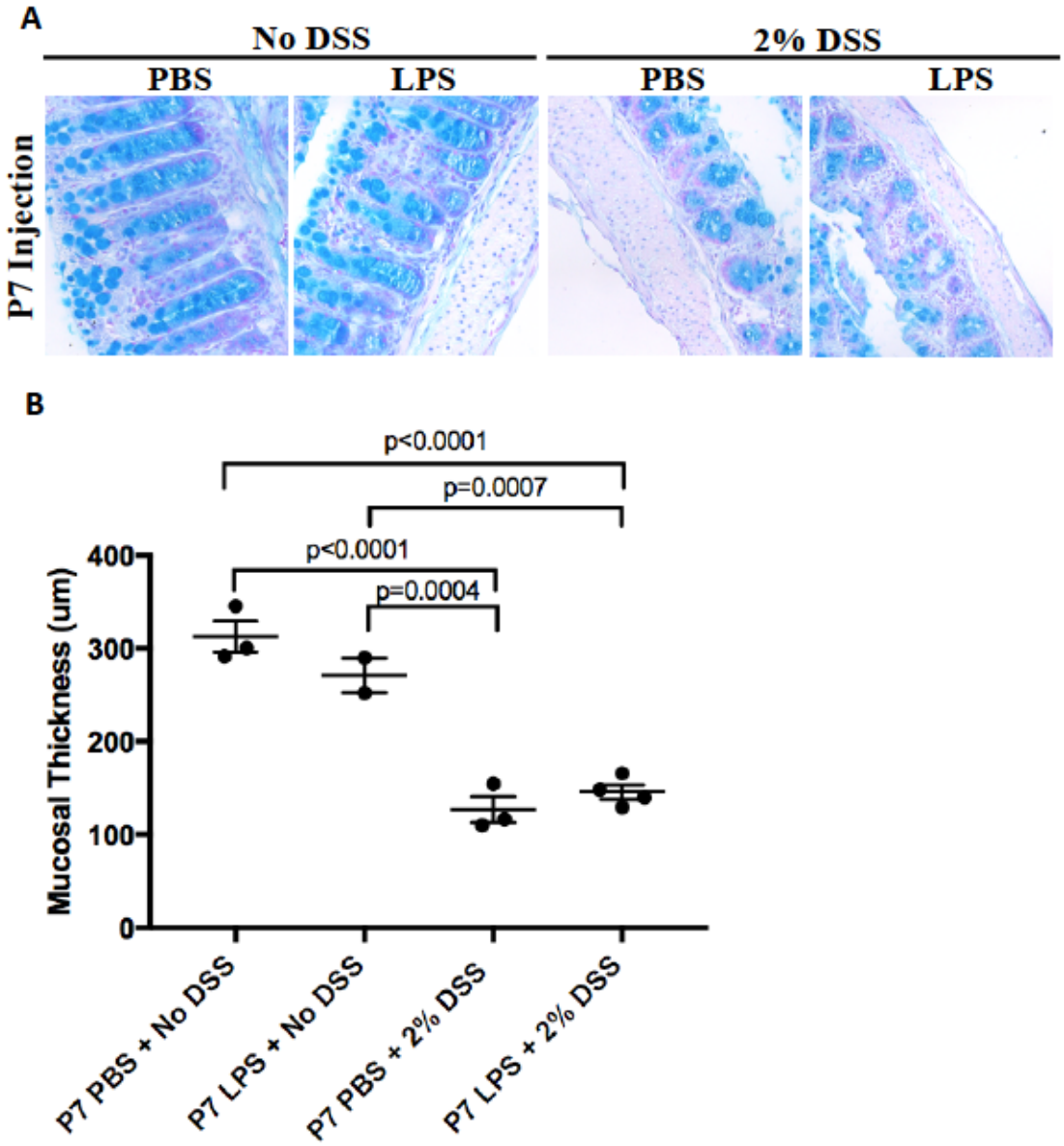

Figure 5.11. ***Postnatal LPS exposure leads to typical loss of tight junctions in adult mice associated with experimental colitis.*** **(A)** Representative confocal micrographs of the colonic epithelium of 6 week old mice that were exposed LPS (2 mg/kg) or PBS at P7 and subsequently exposed to no colitis or to 2% DSS colitis as indicated. **(B)** Quantification of relative fluorescence measurements of ZO-1 staining compared against DAPI staining. $n \geq 6$ per group. All data is representative of three separate experiments and one-way ANOVA tests were performed to determine significance.

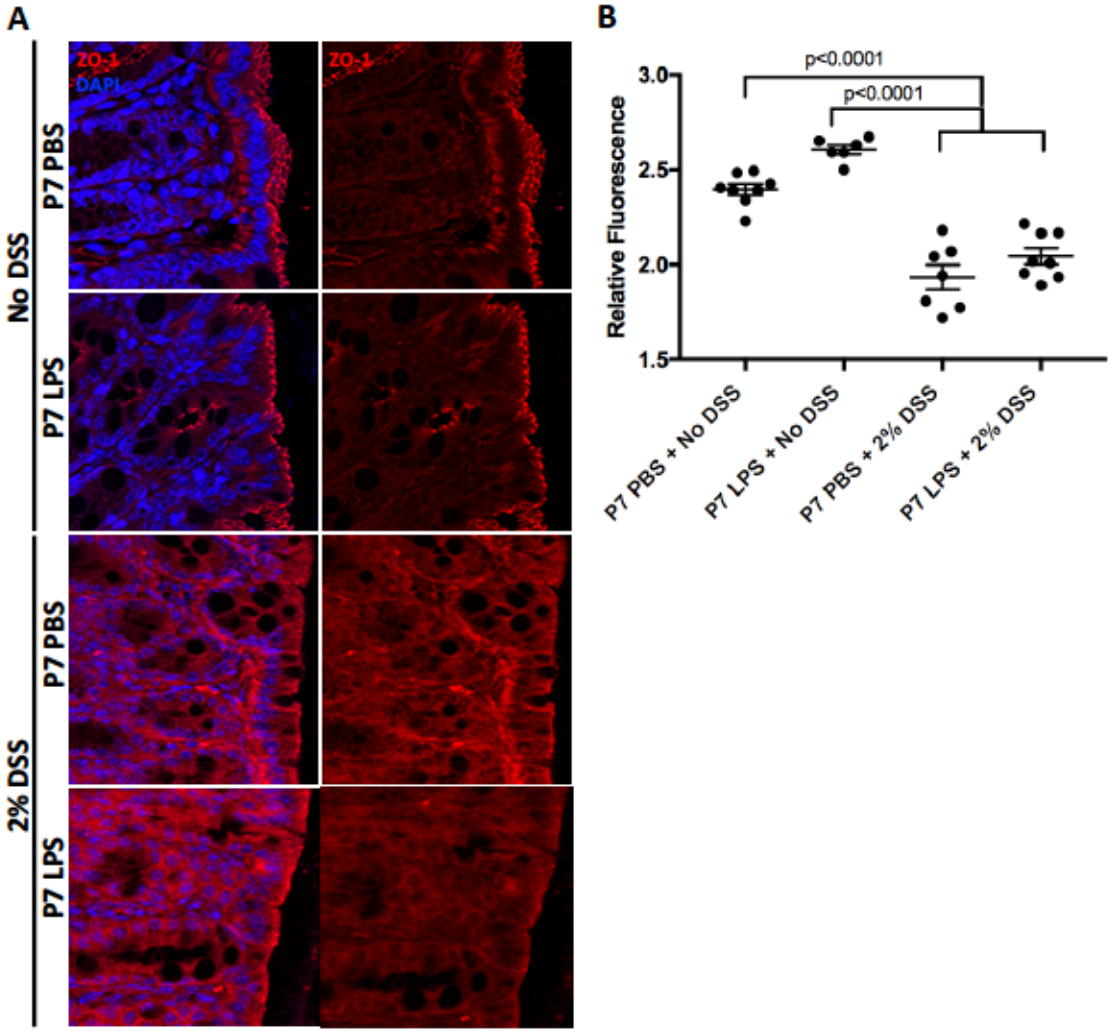

Figure 5.12. ***Effects of in utero LPS exposure on 16S rRNA sequencing of the microbiome.*** (**A**) Diversity analysis using unweighted UniFrac and Bray-Curtis dissimilarity analyses of 6 week old mice across all groups. (**B**) Analysis of alpha diversity amongst each exposure group. (**C-D**) Percent abundance of *Firmicutes* (**C**) and *Flavobacteria* (**D**) in 6 week old mice exposed to LPS (2mg/kg) or PBS *in utero*. 16S rRNA sequencing of stool collected from each exposure group. N=2 for all groups. All data is representative of three separate experiments and t-tests were performed to determine significance.

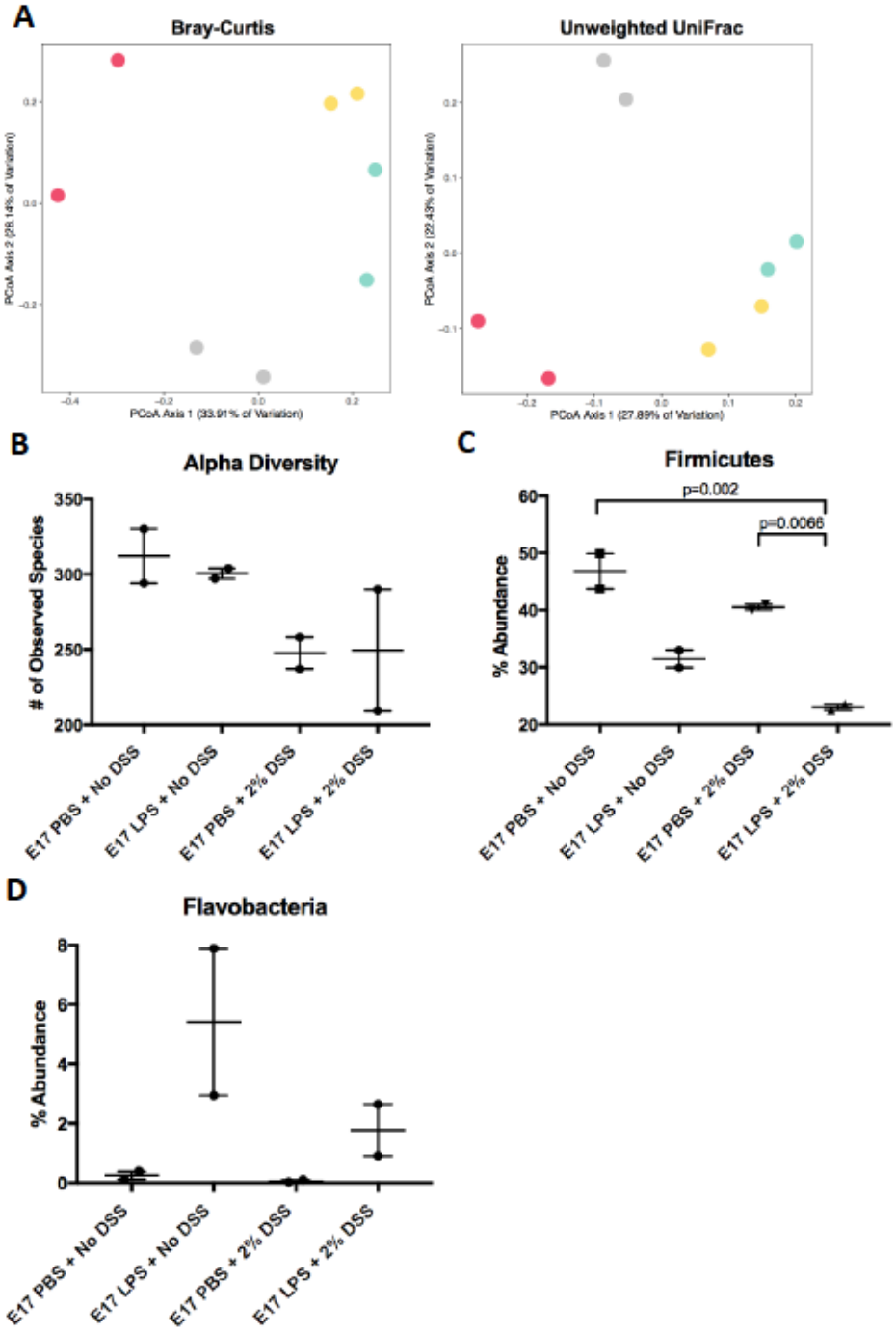

: '#7.!KA@A3&%/3+#4+/1#0#5%&9#+#Dd#@OO#/G9*+43/#>bPKA)b#/G9/3&%/(,+J#
#

Primer	Species	Forward Sequence	Reverse Sequence	Amplicon Size (bp)
RPL0	Mouse/Rat/Human	GGCGACCTGGAAGTCCAACT	CCATCAGCACCACAGCCTTC	143
IL-6	Mouse/Rat	CCAATTTCCAATGCTCTCCT	ACCACAGTGAGGAATGTCCA	182
IL1β	Mouse/Rat	AGTGTGGATCCCAAGCAATACCCA	TGTCCTGACCACTGTTGTTTCCCA	175
TNFα	Mouse/Rat	TTCCGAATTCACTGGAGCCTCGAA	TGCACCTCAGGGAAGAATCTGGAA	144
Tlr4	Mouse	TTTATTCAGAGCCGTTGGTG	CAGAGGATTGTCCTCCCATT	186
Cldn1	Mouse/Rat	ATGCCAGGTATGAATTTGGCCAGG	ATAAGGCCGTGGTGTTGGGTAAGA	131
Muc2	Mouse	TAGTGGAGATTGTGCCGCTGAAGT	AGAGCCCATCGAAGGTGACAAAGT	168

Discussion

The current findings support our initial hypothesis that *in utero* exposure to LPS influences the subsequent development of colitis in the adult. Specifically, we have now shown that mice exposed in utero at E17 to LPS increased *Muc2* expression, increased mucosal thickness, decreased *Tlr4,* and decreased *IL1β,* Tnfα, and IL-6 expression compared to E17 PBS plus DSS exposed mice. Mice exposed to DSS that were exposed to LPS at E17 reveal minimal goblet cell and tight junction loss and showed no signs of colonic injury at colonoscopy, as well as reduced alpha diversity. Reduced alpha diversity is consistent with the notion that E17 LPS-exposed mice received adequate DSS exposure to cause disease though no cellular or inflammatory evidence of disease was found, as both DSS exposure and ulcerative colitis flare-ups are characterized by a reduction in alpha diversity of the microbiome [61]. It is noteworthy that mice that were exposed to PBS *in utero* had a significant increase in *Firmicutes* compared to mice treated *in utero* with LPS, regardless of whether they were exposed to DSS later in life. Taken together, these findings reveal a critical window for LPS exposure in utero for protection against the subsequent development of colitis. It is tempting to speculate that given our recent description that the in utero activation of TLR4 regulates goblet cell differentiation through *Math1* signaling the early exposure to LPS could have long lasting effects on goblet cell production which we now identify [62].

The results suggest that *in utero* environment represents a critical period of vulnerability in the development of the intestinal immune system. Ulcerative colitis has been shown experimentally to be caused by a variety of factors, one of which is dysregulation of the immune system [1,3]. In the healthy intestine, the intestinal

epithelium serves as a selectively permeable barrier, protecting tissue from pathogens that populate the lumen upon ingestion, absorbing nutrients from ingested food, and allowing the transfer of fluids and electrolytes between the tissue and lumen [23,24,63]. Barrier integrity is achieved via the function of the intestinal epithelial cells, which surround the lumen of the colon and secrete mucin via MUC2 that acts as both a lubricant and is home to the intestinal microbiota, and tight junctions, which allow for selective passage of nutrients through the intestinal barrier [23–25]. However, in ulcerative colitis, the intestine loses its selective permeability, instead allowing microbial pathogens to impact the colon and subsequently cause inflammation. Epithelial breakdown is also due, in part, to a loss of tight junctions due to a decrease in the number of ZO-1 proteins present in the tissue and reduced goblet cell function via decreased expression of *mucin 2 (MUC2)* [23,27]. *In utero* LPS exposure could protect the colon from this breakdown by causing a response similar to endotoxin tolerance, in which the immune system does not mount a typical attack on an inflammatory agent because it has previously been exposed to the agent [39,42]. A more restrained immune response could then protect the epithelium from breaking down in the setting of subsequent colitis.

Though usually a symbiotic relationship, alterations in microbiotic diversity can lead to intestinal inflammation [1,7]. Overall, ulcerative colitis is characterized by a decrease in alpha diversity, a measure of species richness and diversity, as well as an increase in populations of beneficial bacteria and a decrease in populations of harmful bacteria in the colon [1,29,31,64]. This reduction in alpha diversity was seen in our experiments among mice that received DSS exposure, regardless of their *in utero* exposure. We also observed a significant decrease in *Firmicutes* populations in both

groups that received E17 LPS exposure. This is consistent with previous literature that found that increased *Firmicutes* levels are associated with reduced GLP-2. Reduced GLP-2 has been shown to be associated with worse colonic injury in a DSS mouse model due to a breakdown of the intestinal barrier. Interestingly, we also saw a significant increase in the abundance of amongst all mice exposed to E17 LPS. In 2016, Jiae, Hwang, and Cho demonstrated that a member of the genus *Flavobacterium*, *Chryseobacterium* sp., induces immune tolerance when injected into the gut, though there is little evidence that this genus has an effect on organisms other than freshwater fish [65]. In addition to a decrease in *MUC2* expression, epithelial breakdown also occurs when levels of glucagon-like peptide 2 (GLP-2), an intestinal epithelium growth factor responsible for barrier maintenance and prevention of LPS accumulation, are decreased. Changes in the number of *Bacteroides* and *Firmicutes,* two of the four major phyla within the gut microbiome, have been linked to reduced GLP-2 levels. Exposure to LPS *in utero* could alter these populations and cause a cascading effect in which *Bacteroides* increases in abundance and *Firmicutes* decreases in abundance. This would then increase GLP-2 levels and reduce intestinal permeability and overall LPS concentration, as LPS would not be able to cross the epithelial barrier. Increased barrier function would reduce any potential inflammatory response via *TLR4* and, subsequently, NF-kB expression. We therefore postulate that prenatal LPS exposure has a direct effect on the makeup of the microbiome, which impacts the protective effects described above.

In aggregate, the current findings support the notion that *in utero* LPS exposure protects mice from developing ulcerative colitis after exposure to experimental colitis. This protective effect may be due to changes in the microbiome that lead to tissue

protection via immune tolerance, or to direct effects on the mucosal epithelium. The approach used in this study can contribute to the growing body of work surrounding the effect of prenatal bacterial exposure on postnatal immune function. It is hoped that through a focus on maternal-fetal interactions during a vulnerable window of mucosal development, we can gain insights into the processes leading to the development of IBD, and thus develop novel therapeutic approaches against disease.

Chapter 6

Conclusions and Future Directions

Summary of significant findings

We conclude that prenatal exposure to LPS primes the postnatal intestine to develop endotoxin tolerance shortly after birth, with the effect slowly disappearing by ten days of age. Though the exact mechanism of endotoxin tolerance remains unknown, *in utero* exposure to LPS likely causes gene expression changes in the MyD88-dependent TLR4 pathway during postnatal bacterial colonization of the gastrointestinal tract, causing a downstream reduction in a variety of inflammatory signals in mice. We also conclude that *in utero* LPS exposure does not have an effect on the severity of NEC in mice, as there was no significant difference in inflammation or tissue structure between mice given LPS and those given PBS prenatally. Because the onset of NEC remains difficult to predict, these negative results help to eliminate localized prenatal bacterial exposure as a potential driver of disease. We further conclude that *in utero* LPS exposure protects mice from developing ulcerative colitis after exposure to a six-day DSS model due to the maintenance of barrier function and muted immune response among these mice. This may be due to changes in the microbiome that lead to tissue protection via immune tolerance. Together, the approaches used in this study can contribute to the growing body of work surrounding the effect of prenatal bacterial exposure on postnatal immune function in the gastrointestinal tract.

Future directions

Though we have explored a variety of postnatal effects after *in utero* LPS exposure, there are key questions that, if answered, would provide further insight into the mechanisms driving the role of this critical exposure window in disease development. The central question surrounding the experiments described in **Chapters 3-5** is the role of epigenetic modifications due to LPS exposure *in utero* and their subsequent effects on disease. Takahaski *et al*. found that DNA methylation and histone deacetylation, which often work in tandem to regulate gene expression, of the 5' region of *TLR4* were both significantly increased among cells that were hypo-responsive to LPS [66]. This provides potential insights into the gene expression changes seen in **Chapters 3-5**. However, *in vitro* experiments do not always have a direct correlation to *in vivo* findings and it would be beneficial to perform similar experiments using chromatin immunoprecipitation, DNA methyltransferase inhibitors, and histone deacetylase on tissue from our intrauterine injection model.

In **Chapter 3**, we showed that prenatal LPS exposure led to endotoxin tolerance upon postnatal LPS exposure at P1. A surprising result of this study was the significant increase in cell proliferation among these mice. This finding, along with our other relevant results, indicate a potential change in gene expression, directing cells within the ileum to new functions. Future flow cytometry experiments to determine which cells are proliferating can help to characterize the cell types involved in the induction of endotoxin tolerance.

An obvious limitation to further studies is the use of CD-1 mice in our experiments, as they are less frequently used in the generation of knockout mice.

However, the option of generating a tight junction or other inflammatory bowel disease-related knockout mouse using CRISPR-Cas9 is fitting for this strain. CRISPR-Cas9 requires a large number of embryos, often produced by use of equine chorionic gonadotropin, in order to generate a knockout mouse [67]. After ovulation, a complete CRISPR-Cas9 plasmid is injected into each zygote, generating the desired knockout [67]. Because CD-1 mice regularly have 12-16 pups per litter, the number of potential knockouts generated from each litter after superovulation is potentially much greater than that of an inbred strain like C57BL/6 or 129/Sv [68]. In the latter strains, tight junction knockouts are generated by deleting exons within genes that code for claudin integral membrane family proteins, which are key components of epithelial tight junctions [69,70]. As such, knocking out these same genes (e.g. *Cldn4*) within CD-1 mice would allow us to further study the effect of *in utero* LPS exposure on tissue integrity and ulcerative colitis development, as our results indicate that this exposure would cause worse disease among knockout mice. A similar pattern is anticipated among *Tlr4* and *Muc2* knockout mice, as both genes have proven to be an integral part of disease both in our studies and in the general ulcerative colitis literature.

Bibliography

[1] J.M. Shapiro, S. Subedi, N.S. LeLeiko, Inflammatory Bowel Disease, Pediatr. Rev. 37 (2016) 337–347. doi:10.1542/pir.2015-0110.

[2] Q. Guan, A Comprehensive Review and Update on the Pathogenesis of Inflammatory Bowel Disease, J. Immunol. Res. 2019 (2019) 1–16.

[3] T. Sairenji, K.L. Collins, D. V. Evans, An Update on Inflammatory Bowel Disease, Prim. Care Clin. Off. Pract. 44 (2017) 673–692. doi:10.1016/J.POP.2017.07.010.

[4] B. Khor, A. Gardet, R.J. Xavier, Genetics and pathogenesis of inflammatory bowel disease, Nature. 474 (2011) 307–317. doi:10.1038/nature10209.

[5] G. Pasternak, D. Aebisher, R. Filip, D. Bartusik-Aebisher, Inflammatory bowel disease: clinical aspects, Eur. J. Clin. Exp. Med. 16 (2019) 341–345. doi:10.15584/ejcem.2018.4.12.

[6] S.K.F. Chong, A.J. Blackshaw, S. Boyle, C.B. Williams, J.A. Walker-Smith, Histological diagnosis of chronic inflammatory bowel disease in childhood, Gut. 26 (1985) 55–59. doi:10.1136/gut.26.1.55.

[7] S.R. Brant, Update on the heritability of inflammatory bowel disease: The importance of twin studies, Inflamm. Bowel Dis. 17 (2011) 1–5. doi:10.1002/ibd.21385.

[8] S.M. Ho, J.D. Lewis, E.A. Mayer, S.E. Plevy, E. Chuang, S.M. Rappaport, et al., Challenges in IBD Research: Environmental Triggers, Inflamm. Bowel Dis. 25 (2019) S13–S23. doi:10.1093/ibd/izz076.

[9] P.L. Lakatos, Environmental factors affecting inflammatory bowel disease: Have we made progress?, Dig. Dis. 27 (2009) 215–225. doi:10.1159/000228553.

[10] E.A. Rhee, Sang H, Pothoulakis, C and Mayer, Nat. Rev. Gastroenterol. Hepatol. 6 (2009) 306–314. doi:10.1038/nrgastro.2009.35.Principles.

[11] A.N. Ananthakrishnan, Epidemiology and risk factors for IBD, Nat. Rev. Gastroenterol. Hepatol. 12 (2015) 205–217. doi:10.1038/nrgastro.2015.34.

[12] S.C. Ng, S. Woodrow, N. Patel, J. Subhani, M. Harbord, Role of genetic and environmental factors in British twins with inflammatory bowel disease, Inflamm. Bowel Dis. 18 (2012) 725–736. doi:10.1002/ibd.21747.

[13] S.C. Ng, H.Y. Shi, N. Hamidi, F.E. Underwood, W. Tang, E.I. Benchimol, et al., Worldwide incidence and prevalence of inflammatory bowel disease in the 21st century: a systematic review of population-based studies, Lancet. 390 (2017) 2769–2778. doi:10.1016/S0140-6736(17)32448-0.

[14] N.A. Molodecky, I.S. Soon, D.M. Rabi, W.A. Ghali, M. Ferris, G. Chernoff, et al., Increasing incidence and prevalence of the inflammatory bowel diseases with time, based on systematic review, Gastroenterology. 142 (2012) 46-54.e42. doi:10.1053/j.gastro.2011.10.001.

[15] J. Cosnes, C. Gowerrousseau, P. Seksik, A. Cortot, Epidemiology and natural history of inflammatory bowel diseases, Gastroenterology. 140 (2011) 1785-1794.e4. doi:10.1053/j.gastro.2011.01.055.

[16] J.-M. Zhang, J. An, Cytokines, Inflammation and Pain, Int Anesth. Clin. 69 (2009) 482–489. doi:10.1097/AIA.0b013e318034194e.Cytokines.

[17] D.Q. Shih, S.R. Targan, D. McGovern, Recent advances in IBD pathogenesis:

Genetics and immunobiology, Curr. Gastroenterol. Rep. 10 (2008) 568–575. doi:10.1007/s11894-008-0104-x.
[18] L. Zhu, J. Han, L. Li, Y. Wang, Y. Li, S. Zhang, Claudin family participates in the pathogenesis of inflammatory bowel diseases and colitis-associated colorectal cancer, Front. Immunol. 10 (2019) 1–11. doi:10.3389/fimmu.2019.01441.
[19] C.A. Anderson, G. Boucher, C.W. Lees, A. Franke, M. D'Amato, K.D. Taylor, et al., Meta-analysis identifies 29 additional ulcerative colitis risk loci, increasing the number of confirmed associations to 47, Nat. Genet. 43 (2011) 246–252. doi:10.1038/ng.764.
[20] Y. Lu, X. Li, S. Liu, Y. Zhang, D. Zhang, Toll-like receptors and inflammatory bowel disease, Front. Immunol. 9 (2018) 1–9. doi:10.3389/fimmu.2018.00072.
[21] Y. Toiyama, T. Araki, S. Yoshiyama, J.I. Hiro, C. Miki, M. Kusunoki, The expression patterns of toll-like receptors in the ileal pouch mucosa of postoperative ulcerative colitis patients, Surg. Today. 36 (2006) 287–290. doi:10.1007/s00595-005-3144-y.
[22] T. Oshima, H. Miwa, T. Joh, Changes in the expression of claudins in active ulcerative colitis, J. Gastroenterol. Hepatol. 23 (2008) 3–7. doi:10.1111/j.1440-1746.2008.05405.x.
[23] P. Henderson, J.E. Van Limbergen, J. Schwarze, D.C. Wilson, Function of the intestinal epithelium and its dysregulation in inflammatory bowel disease, Inflamm. Bowel Dis. 17 (2011) 382–395. doi:10.1002/ibd.21379.
[24] R. Okumura, K. Takeda, Roles of intestinal epithelial cells in the maintenance of gut homeostasis, Exp. Mol. Med. 49 (2017) e338-8. doi:10.1038/emm.2017.20.
[25] L.W. Peterson, D. Artis, Intestinal epithelial cells: Regulators of barrier function and immune homeostasis, Nat. Rev. Immunol. 14 (2014) 141–153. doi:10.1038/nri3608.
[26] T. Kucharzik, C. Maaser, A. Lügering, M. Kagnoff, L. Mayer, S. Targan, et al., Recent understanding of IBD pathogenesis: Implications for future therapies, Inflamm. Bowel Dis. 12 (2006) 1068–1082. doi:10.1097/01.mib.0000235827.21778.d5.
[27] M.E.V. Johansson, J.M. Holmén Larsson, G.C. Hansson, The two mucus layers of colon are organized by the MUC2 mucin, whereas the outer layer is a legislator of host-microbial interactions, Proc. Natl. Acad. Sci. U. S. A. 108 (2011) 4659–4665. doi:10.1073/pnas.1006451107.
[28] A. Nishida, R. Inoue, O. Inatomi, S. Bamba, Y. Naito, A. Andoh, Gut microbiota in the pathogenesis of inflammatory bowel disease, Clin. J. Gastroenterol. 11 (2018) 1–10. doi:10.1007/s12328-017-0813-5.
[29] Z.H. Shen, C.X. Zhu, Y.S. Quan, Z.Y. Yang, S. Wu, W.W. Luo, et al., Relationship between intestinal microbiota and ulcerative colitis: Mechanisms and clinical application of probiotics and fecal microbiota transplantation, World J. Gastroenterol. 24 (2018) 5–14. doi:10.3748/wjg.v24.i1.5.
[30] A.T. Abegunde, B.H. Muhammad, O. Bhatti, T. Ali, Environmental risk factors for inflammatory bowel diseases: Evidence based literature review, World J. Gastroenterol. 22 (2016) 6296–6317. doi:10.3748/wjg.v22.i27.6296.
[31] M. Derrien, C. Belzer, W.M. de Vos, Akkermansia muciniphila and its role in regulating host functions, Microb. Pathog. 106 (2017) 171–181.

doi:10.1016/j.micpath.2016.02.005.
[32] H. Earley, G. Lennon, Á. Balfe, J.C. Coffey, D.C. Winter, P.R. O'Connell, The abundance of Akkermansia muciniphila and its relationship with sulphated colonic mucins in health and ulcerative colitis, Sci. Rep. 9 (2019) 1–9. doi:10.1038/s41598-019-51878-3.
[33] T.D. Schaible, R.A. Harris, S.E. Dowd, C.W. Smith, R. Kellermayer, S.A. Mir, et al., Prenatal methyl-donor supplementation augments colitis in young adult mice, Hum. Mol. Genet. 20 (2011) 1687–1696. doi:10.1093/hmg/ddr044.
[34] T.D. Schaible, R.A. Harris, S.E. Dowd, C.W. Smith, R. Kellermayer, Maternal methyl-donor supplementation induces prolonged murine offspring colitis susceptibility in association with mucosal epigenetic and microbiomic changes, Hum. Mol. Genet. 20 (2011) 1687–1696. doi:10.1093/hmg/ddr044.
[35] A. Olin, E. Henckel, Y. Chen, T. Lakshmikanth, C. Pou, J. Mikes, et al., Stereotypic Immune System Development in Newborn Children, Cell. 174 (2018) 1277-1292.e14. doi:10.1016/j.cell.2018.06.045.
[36] Y.C. Lu, W.C. Yeh, P.S. Ohashi, LPS/TLR4 signal transduction pathway, Cytokine. 42 (2008) 145–151. doi:10.1016/j.cyto.2008.01.006.
[37] S.J.H. Van Deventer, H.R. Buller, J.W. Ten Cate, L.A. Aarden, C.E. Hack, A. Sturk, Experimental endotoxemia in humans: Analysis of cytokine release and coagulation, fibrinolytic, and complement pathways, Blood. 76 (1990) 2520–2526. doi:10.1182/blood.v76.12.2520.bloodjournal76122520.
[38] M.A. West, W. Heagy, Endotoxin tolerance: A review, 30 (2002).
[39] O.M. Pena, J. Pistolic, D. Raj, C.D. Fjell, R.E.W. Hancock, Endotoxin Tolerance Represents a Distinctive State of Alternative Polarization (M2) in Human Mononuclear Cells, J. Immunol. 186 (2011) 7243–7254. doi:10.4049/jimmunol.1001952.
[40] J.M. Cavaillon, M. Adib-Conquy, Bench-to-bedside review: Endotoxin tolerance as a model of leukocyte reprogramming in sepsis, Crit. Care. 10 (2006) 1–8. doi:10.1186/cc5055.
[41] S.E. Greisman, E.J. Young, W.E. Woodward, Mechanisms of Endotoxin Tolerance, J. Exp. Med. 124 (1966) 983–1000. doi:10.1084/jem.124.5.983.
[42] D. Liu, S. Cao, Y. Zhou, Y. Xiong, Recent advances in endotoxin tolerance, J. Cell. Biochem. 120 (2019) 56–70. doi:10.1002/jcb.27547.
[43] N. Hirohashi, D.C. Morrison, Low-dose lipopolysaccharide (LPS) pretreatment of mouse macrophages modulates LPS-dependent interleukin-6 production in vitro, Infect. Immun. 64 (1996) 1011–1015. doi:10.1128/iai.64.3.1011-1015.1996.
[44] S. Flohe, E.D. Ferna, M. Ackermann, T. Hirsch, J. Bo, F.U. Schade, Endotoxin Tolerance in Rats : Hsp 70 in Lung and Liver During Endotoxin Shock, October. 11 (1999) 796–804. doi:10.1006/cyto.1998.0490.
[45] F. Nomura, S. Akashi, Y. Sakao, S. Sato, T. Kawai, M. Matsumoto, et al., Cutting Edge: Endotoxin Tolerance in Mouse Peritoneal Macrophages Correlates with Down-Regulation of Surface Toll-Like Receptor 4 Expression, J. Immunol. 164 (2000) 3476–3479. doi:10.4049/jimmunol.164.7.3476.
[46] D.F. Niño, C.P. Sodhi, D.J. Hackam, Necrotizing enterocolitis: New insights into pathogenesis and mechanisms, Nat. Rev. Gastroenterol. Hepatol. 13 (2016) 590–600. doi:10.1038/nrgastro.2016.119.

[47] E. Claud, Neonatal Necrotizing Enterocolitis – Inflammation and Intestinal Immaturity, Antiinflamm. Antiallergy. Agents Med. Chem. 8 (2009) 248–259. doi:10.2174/187152309789152020.
[48] D.J. Hackam, A. Afrazi, M. Good, C.P. Sodhi, Innate immune signaling in the pathogenesis of necrotizing enterocolitis, Clin. Dev. Immunol. 2013 (2013). doi:10.1155/2013/475415.
[49] D.J. Hackam, C.P. Sodhi, Toll-Like Receptor–Mediated Intestinal Inflammatory Imbalance in the Pathogenesis of Necrotizing Enterocolitis, Cmgh. 6 (2018) 229-238.e1. doi:10.1016/j.jcmgh.2018.04.001.
[50] I. Burd, J. Chai, J. Gonzalez, E. Ofori, H. Monnerie, P.D. Le Roux, et al., Beyond white matter damage: fetal neuronal injury in a mouse model of preterm birth, Am. J. Obstet. Gynecol. 201 (2009) 279.e1-279.e8. doi:10.1016/j.ajog.2009.06.013.
[51] M.M.C. Andrade, S.S.K. Ariga, D.F. Barbeiro, H. V. Barbeiro, R.N. Pimentel, R.C. Petroni, et al., Endotoxin tolerance modulates TREG and TH17 lymphocytes protecting septic mice, Oncotarget. 10 (2019) 3451–3461. doi:10.18632/oncotarget.26919.
[52] M. Good, C.P. Sodhi, Y. Yamaguchi, H. Jia, P. Lu, W.B. Fulton, et al., The human milk oligosaccharide 2′-fucosyllactose attenuates the severity of experimental necrotising enterocolitis by enhancing mesenteric perfusion in the neonatal intestine, Br. J. Nutr. 116 (2016) 1175–1187. doi:10.1017/S0007114516002944.
[53] D. Lu, Peng, Sodhi, Chhinder P., Jia, Hongpeng, Shaffiey, Shahab, Good, Misty, Branca, Maria F., Hackam, Animal models of gastrointestinal and liver diseases. Animal models of necrotizing enterocolitis: pathophysiology, translational relevance, and challenges., Am. J. Physiol. - Gastrointest. Liver Physiol. 306 (2014) G917–G928.
[54] C.E. Egan, C.P. Sodhi, M. Good, J. Lin, H. Jia, Y. Yamaguchi, et al., Hackam Lymphcyte NEC 2016, 126 (2016) 495–508. doi:10.1172/JCI83356.on.
[55] Y.E. Kim, M. Lee, H. Gu, J. Kim, S. Jeong, S. Yeo, et al., HIF-1α activation in myeloid cells accelerates dextran sodium sulfate-induced colitis progression in mice, Dis. Model. Mech. 11 (2018). doi:10.1242/dmm.033241.
[56] Y.H. Park, N. Kim, Y.K. Shim, Y.J. Choi, R.H. Nam, Y.J. Choi, et al., Adequate Dextran Sodium Sulfate-induced Colitis Model in Mice and Effective Outcome Measurement Method, J. Cancer Prev. 20 (2015) 260–267. doi:10.15430/jcp.2015.20.4.260.
[57] D.J. Sodhi, Chhinder P., Neal, Matthew D., Siggers, Richard, Sho, Shonan, Ma, Congrong, Branca, Maria, Prindle Jr., Thomas, Russo, Anthony M., Afrazi, Amin, Good, Misty, Brower-Sinning, Rachel, Firek, Brian, Morowitz, Michael J., Ozolek, John A., Gittes, Georg, Intestinal Epithelial Toll-Like Receptor 4 Regulates Goblet Cell Development and Is Required for Necrotizing Enterocolitis in Mice, Gastroenterology. 143 (2012) 708–718. doi:10.1038/jid.2014.371.
[58] Håkansson, N. Tormo-Badia, A. Baridi, J. Xu, G. Molin, M.L. Hagslätt, et al., Immunological alteration and changes of gut microbiota after dextran sulfate sodium (DSS) administration in mice, Clin. Exp. Med. 15 (2014) 107–120. doi:10.1007/s10238-013-0270-5.
[59] N. a Nagalingam, J.Y. Kao, V.B. Young, Microbial ecology of the murine gut associated with the development of DSS-colitis, Imflammatory Bowel Dis. 17

(2012) 917–926. doi:10.1002/ibd.21462.Microbial.
[60] J. Hansen, A. Gulati, R.B. Sartor, The role of mucosal immunity and host genetics in defining intestinal commensal bacteria, Curr. Opin. Gastroenterol. 26 (2010) 564–571. doi:10.1097/MOG.0b013e32833f1195.
[61] C.J. Kiely, P. Pavli, C.L. O'Brien, The role of inflammation in temporal shifts in the inflammatory bowel disease mucosal microbiome, Gut Microbes. 9 (2018) 477–485. doi:10.1080/19490976.2018.1448742.
[62] D.J. Sodhi, Chhinder P., Neal, Matthew D., Siggers, Richard, Sho, Shonan, Ma, Congrong, Branca, Maria, Prindle Jr., Thomas, Russo, Anthony M., Afrazi, Amin, Good, Misty, Brower-Sinning, Rachel, Firek, Brian, Morowitz, Michael J., Ozolek, John A., Gittes, Georg, Intestinal Epithelial Toll-Like Receptor 4 Regulates Goblet Cell Development and Is Required for Necrotizing Enterocolitis in Mice, Gastroenterology. 143 (2012) 708–718. doi:10.1038/jid.2014.371.
[63] Q. Guan, Review Article A Comprehensive Review and Update on the Pathogenesis of Inflammatory Bowel Disease, 2019 (2019).
[64] H. Earley, G. Lennon, Á. Balfe, J.C. Coffey, D.C. Winter, P.R. O'Connell, The abundance of Akkermansia muciniphila and its relationship with sulphated colonic mucins in health and ulcerative colitis, Sci. Rep. 9 (2019). doi:10.1038/s41598-019-51878-3.
[65] J. Lee, S. Hwang, S. Cho, Immune tolerance to an intestine-adapted bacteria, Chryseobacterium sp., injected into the hemocoel of Protaetia brevitarsis seulensis, Sci. Rep. 6 (2016). doi:10.1038/srep31722.
[66] K. Takahashi, Y. Sugi, A. Hosono, S. Kaminogawa, Epigenetic Regulation of TLR4 Gene Expression in Intestinal Epithelial Cells for the Maintenance of Intestinal Homeostasis, J. Immunol. 183 (2009) 6522–6529. doi:10.4049/jimmunol.0901271.
[67] Y. Nakagawa, T. Sakuma, N. Nishimichi, Y. Yokosaki, N. Yanaka, T. Takeo, et al., Ultra-superovulation for the CRISPR-Cas9-mediated production of gene-knockout, single-amino-acid-substituted, and floxed mice, Biol. Open. 5 (2016) 1142–1148. doi:10.1242/bio.019349.
[68] C.R. Laboratories, Charles River Laboratories Technical Bulletin 1999, 1999.
[69] M. Furuse, M. Hata, K. Furuse, Y. Yoshida, A. Haratake, Y. Sugitani, et al., Claudin-based tight junctions are crucial for the mammalian epidermal barrier: A lesson from claudin-1-deficient mice, J. Cell Biol. 156 (2002) 1099–1111. doi:10.1083/jcb.200110122.
[70] H. Kage, P. Flodby, D. Gao, Y.H. Kim, C.N. Marconett, L. Demaio, et al., Claudin 4 knockout mice: Normal physiological phenotype with increased susceptibility to lung injury, Am. J. Physiol. - Lung Cell. Mol. Physiol. 307 (2014) L524–L536. doi:10.1152/ajplung.00077.2014.

Emilyn C. Banfield

701 Cathedral Street, Apt 41 Baltimore, MD 21201
407-739-6172 || ebanfie1@jhmi.edu

Education

PhD, Human Genetics, Johns Hopkins University School of Medicine **May 2020**
Thesis Topic: "The role of *in utero* endotoxin exposure in inflammatory bowel disease development in mice"
Mentor: David Hackam, MD, PhD

MPH, Epidemiology, University of Texas School of Public Health **May 2015**
Thesis Topic: "The role of *ERCC2* DNA methylation on survival among pediatric medulloblastoma patients"
Mentors: Laura Mitchell, PhD, Philip Lupo, PhD

BS, Genetics, Clemson University **Dec 2012**

Positions and Academic Appointments

Teaching Assistant Aug 2017-Aug 2019
Department of Pathology, JHU School of Medicine
Course: Pathobiology for Graduate Students

Guest Lecturer Sept 4, 2019
Department of Psychology, Johns Hopkins University
Course: Introduction to Developmental Psychology, Genetics and Heritability Lecture

Graduate Research Assistant Aug 2014-May 2015
Department of Epidemiology, MD Anderson Cancer Center
Mentors: Dr. Shine Chang, Dr. Alexis Frazier-Wood

Cancer Prevention Research Training Program May 2014-Aug 2014
MD Anderson Cancer Center
Mentors: Dr. Shine Chang, Dr. Alexis Frazier-Wood

Undergraduate Research Assistant Aug 2011-Dec 2012
Clemson University
Mentor: Dr. Leigh Anne Clark, Canine Genetics Lab

Undergraduate Research Assistant May 2012-Dec 2012
Clemson University Genomics Institute (CUGI)
Director: Dr. Christopher Saski

Publications

Banfield, E., Liu, Y., Davis, J.S., Chang, S. & Frazier-Wood, A.C. Poor adherence to US dietary guidelines for children and adolescents in the NHANES 2005-2010 population. Journal of the Academy of Nutrition and Dietetics. 2015, Sept; S2212-2672(15)01259-9. doi: 10.1016/j.jand.2015.08.010.

Banfield, E., Brown, A., Peckham, E.C., Rednam, S.P., Murray, J., Okcu, M., Mitchell, L., Chintagumpala, M.M., Lau, C.C., Scheurer, M. & Lupo, P. Exploratory analysis of *ERCC2* DNA methylation in survival among pediatric medulloblastoma patients. Cancer Epidemiology. 2016, Oct; 44:161-166. doi: 10.1016/j.canep.2016.08.020.

Werts, A., Fulton, W., Saad-Eldin, A., Chen, Y., Kovler, M., Jia, H., **Banfield, E.**, Buck, R., Goerhing, K., Prindle, T., Wang, S., Zhou, Q., Lu P., Yamaguchi, Y., Sodhi, C., & Hackam, D. A novel role for necroptosis in the pathogenesis of necrotizing enterocolitis. Cellular and Molecular Gastroenterology and Hepatology. 2019, November; *Accepted, awaiting publication.*

Davis, J.S., **Banfield, E.**, Lee, H.Y., Peng, H.L., Chang, S. & Frazier-Wood, A.C. Lifestyle behavior patterns and mortality among adults in the NHANES 1988-1994 population: A Latent Profile Analysis. Preventive Medicine. 2019, March; 120:131-139. doi: 10.1016/j.ypmed.2019.01.012.

Davis, J.S., Lee, H.Y., Kim, J., Advani, S.M., Peng, H.L., **Banfield, E.**, Hawk, E.T, Chang, S. & Frazier-Wood, A.C. Use of Non-Steroidal Anti-Inflammatory Drugs in U.S. Adults: Changes Over Time and by Demographic. Open Heart. 2017, April; 4(1):e000550. doi: 10.1136/openhrt-2016-000550.

Commentary

Kim, J., **Banfield, E.**, Davis, J.S., & Chang, S. Comment on "Better Post-Diagnosis Diet Quality Is Associated with Reduced Risk of Death among Postmenopausal Women with Invasive Breast Cancer in the Women's Health Initiative". Breast Diseases, A Year Book Quarterly, 2014. 25(4).

Conference Activity

Talks

Banfield, E. "Prenatal Inflammation Primes the Neonatal Intestine for Endotoxin Tolerance." *American Society of Human Genetics 2018 Annual Meeting*, San Diego, California, October 29, 2018. Platform Talk.

Posters

Banfield, E., Fulton, W., Burd, I., Sodhi, C., & Hackam, D. *In utero* endotoxin exposure decreases subsequent inflammatory bowel disease severity in mice. *American Society of Human Genetics 2019 Annual Meeting*, Houston, Texas, October 16, 2019. Reviewers Choice Abstract.

Banfield, E., Liu, Y., Davis, J.S., Chang, S. & Frazier-Wood, A.C. Poor adherence to US dietary guidelines for children and adolescents in the NHANES 2005-2010 population. *MD Anderson Cancer Prevention Research and Training Summer Exposition,* Houston, Texas, August 5-6, 2014.

Banfield, E.,* Davis, J.S.,* Lee, H.Y., Chang, S. & Frazier-Wood, A.C. A clustering analysis of lifestyle behaviors and their effects on mortality, *American Society of Preventive Oncology 2015 Annual Meeting,* Birmingham, Alabama, March 15, 2015.

Funding

T32 Predoctoral Training Grant — Aug 2015-Jun 2016
Principle Investigator: David Valle

R25E Cancer Research Training Grant
Principle Investigators: Shine Chang, Carrie Cameron — May 2014-Aug 2014

Volunteering

Baltimore County Domestic Violence/Sexual Assault Hotline — May 2019-May 2020
Total Time Volunteered: 55 Hours

Guiding Eyes for the Blind Puppy Raiser — June 2019-Present

President, Women in Science Committee — Jan 2018-July 2019
Johns Hopkins University School of Medicine

Child Life Volunteer — Nov 2016-Mar 2019
Johns Hopkins Bloomberg Children's Hospital
Total Time Volunteered: 310 Hours

Patient Coordinator — May 2012-Dec 2012
Clemson Free Clinic
Total Time Volunteered: 60 Hours

Hand Hygiene Study Surveyor — Apr 2012-Aug 2012
AnMed Health Main Campus Hospital
Total Time Volunteered: 50 Hours

Treasurer, Biochemistry and Genetics Club — Aug 2010-Dec 2012
Clemson University

Honors and Awards

Johns Hopkins School of Medicine Graduate Student Association Travel Award — Oct 2018

Johns Hopkins University Department of Cell Biology Lewis Travel Award — Oct 2018

UT Health Golf Tournament Scholarship — Oct 2014

Lauren and Adam Strauss Endowed Scholarship — Aug 2014

MD Anderson Elevator Speech Competition, Finalist — Aug 2014

Clemson University All-ACC Honor Roll — 2009-2011